Simulation of the Tropical Oceans with an Ocean GCM Coupled to an Atmospheric Mixed-Layer Model

RAGU MURTUGUDDE

Universities Space Research Association, Laboratory for Hydrospheric Processes, NASA/GSFC, Greenbelt, Maryland

RICHARD SEAGER

Lamont-Doherty Earth Observatory of Columbia University, Palisades, New York

ANTONIO BUSALACCHI

Laboratory for Hydrospheric Processes, NASA/GSFC, Greenbelt, Maryland

(Manuscript received 18 September 1995, in final form 2 January 1996)

ABSTRACT

A reduced gravity, primitive equation, ocean general circulation model (GCM) is coupled to an advective atmospheric mixed-layer (AML) model to demonstrate the importance of a nonlocal atmospheric mixed-layer parameterization for a proper simulation of surface heat fluxes and sea surface temperatures (SST). Seasonal variability of the model SSTs and the circulation are generally in good agreement with the observations in each of the tropical oceans. These results are compared to other simulations that use a local equilibrium mixed-layer model. Inclusion of the advective AML model is demonstrated to lead to a significant improvement in the SST simulation in all three oceans. Advection and diffusion of the air humidity play significant roles in determining SSTs even in the tropical Pacific where the local equilibrium assumption was previously deemed quite accurate. The main, and serious, model flaw is an inadequate representation of the seasonal cycle in the upwelling regions of the eastern Atlantic and Pacific Oceans. The results indicate that the feedback between mixed-layer depths and SSTs can amplify SST errors, implying that increased realism in the modeling of the ocean mixed layer increases the demand for realism in the representation of the surface heat fluxes. The performance of the GCM with a local-equilibrium mixed-layer model in the Atlantic is as poor as previous simple ocean model simulations of the Atlantic. The conclusion of earlier studies that the simple ocean model was at fault may, in fact, not be correct. Instead the local-equilibrium heat flux parameterization appears to have been the major source of error. Accurate SST predictions may, hence, be feasible by coupling the AML model to computationally efficient simple ocean models.

1. Introduction

SST is the principal ocean variable that affects the atmosphere. Prediction of the coupled ocean-atmosphere variability will always be limited by our ability to predict SST. To date, a rather impressive operational prediction of interannual variability of the coupled system has been achieved with an extremely simplified heat flux formulation (Cane et al. 1986; Chen et al. 1995). However, there is reason to believe that further improvements will require, among other things, a more realistic treatment of air–sea energy fluxes. State of the art atmospheric models behave reasonably when forced with observed SSTs just as the ocean models reproduce observed SSTs and currents when forced with relaxation conditions on SST and sea surface salinity. However, when these models are coupled to each other, unrealistic flux corrections are necessary for avoiding climate drift in the coupled system. The implication is that one or the other component inadequately represents the feedbacks between surface energy fluxes and the SST. This is hardly surprising since atmosphere and ocean models are rarely verified against the highly uncertain observed estimates of the air–sea heat flux.

One approach to enhancing climate prediction skill is to try to improve the coupled models as a system. Another approach would be to simplify the physics of one component of this coupled system to concentrate on the other component. In this work we couple an ocean general circulation model (GCM) to a thermodynamic model of the lowest level of the atmosphere in an effort to realistically account for the interrelations between the SST and the air–sea heat fluxes. By allowing the ocean model maximum freedom to determine

Corresponding author address: Dr. Ragu Murtugudde, Universities Space Research Association, Code 970, NASA/GSFC, Bldg. 22, Greenbelt, MD 20771.
E-mail: ragu@seetha.gsfc.nasa.gov

its own SST, this allows us to truly address the ocean model's ability to predict SSTs.

While the seasonal variations in surface currents and thermocline movements in the tropics are simulated accurately by several models (e.g., Busalacchi and O'Brien 1980; Philander et al. 1987), simulations of the seasonal cycle of SST leave plenty of room for improvements. In all fairness, determining SST is quite complicated with different processes controling the SST in different regions. For example, in the eastern tropical Pacific, surface heat flux, upwelling, advection, and vertical mixing are all involved in determining SST, although the relative importance of these processes is far from well determined. Ocean modelers have strived to improve SST simulations, but with some justification, often blamed the inadequacies of model SST on the uncertainties in surface heat fluxes. Blumenthal and Cane (1989) concluded that the model deficiencies in the tropical Pacific could not be identified unambiguously due to uncertainties in the forcing data.

Many ocean modelers attempt to avoid the problems introduced by uncertain heat fluxes by using restoring boundary conditions that relax SSTs back to climatology (e.g., Haney 1971; Chang 1994). An alternative is to specify the air temperature and humidity that appear in the bulk formula heat flux parameterizations (e.g., Miller et al. 1992; Giese and Cayan 1993). Many attempts to simulate seasonal and interannual variability in ocean dynamics have also relied on flux corrections (e.g., Oberhuber 1993; Murtugudde et al. 1995) or on idealized heat fluxes (e.g., Latif 1987; Philander and Siegel 1985).

In reality there is a strong feedback between the SST and the air–sea fluxes. The physical process at the center of this feedback is the adjustment of the lowest level of the atmosphere to the underlying SST (e.g., Betts and Ridgway 1989). This occurs because of the tiny heat and moisture storage of the atmospheric boundary layer relative to the upper layers of the ocean. Away from continents the surface atmospheric humidity and air temperature are forced to track the SST (e.g., Cayan 1980). Because this is so, and not the other way around, Seager et al. (1988, SZC hereafter) argued that specifying the air temperature and humidity in the heat flux boundary conditions of an ocean model is equivalent to imposing the SST. While using such restoring boundary conditions may be justified if the main focus of attention is the model dynamics, it is decidedly unhelpful if the aim is to simulate SST: it puts in the answer. Ignoring the adjustment of the low-level atmosphere to the underlying SST inevitably distorts the flux-SST relationship. This can have important ramifications for simulation of natural variability (Seager et al. 1995b; Rahmstorff and Willebrand 1995). It is an excellent idea before coupling an ocean model to an atmosphere model, to test its behavior in a configuration that takes proper account of the flux–SST feedback. This is what we aim to do here.

SZC proposed a heat flux formulation that required only solar radiation, cloud cover, and winds as atmospheric inputs and computed the other terms of the surface heat flux in terms of the SST. This formulation demonstrated considerable skill in reproducing the general features of tropical Pacific SST climatology and variability (Seager 1989) when used with a simple, reduced gravity, ocean model. Using satellite observations of solar radiation, and a more general heat flux formulation, the results were improved further (Seager and Blumenthal 1994) although the seasonal cycle of the SST was phase lagged (probably due to the simplistic mixed-layer physics). The SZC heat flux formulation assumes a one-dimensional balance in the atmospheric planetary boundary layer (PBL) in order to compute the air humidity from SST. This can be valid only in areas of the ocean away from continental margins and strong SST gradients. In other regions, the PBL would not be expected to be in local equilibrium with the underlying ocean. The most obvious example is advection of cold and dry continental air over warm western boundary currents during northern winter. In such cases the SZC heat flux is wholly inappropriate.

To deal with a subtropical analogy, Blumenthal (1990) introduced a model for advection of dry air off West Africa, which acted to cool the SST in the northeastern subtropical Atlantic. A different approach has been presented by Luksch and von Storch (1992), who use an advective model for air temperature anomalies over the North Pacific. Kleeman and Power (1994) have developed an advective model for the total air temperature. Both of those models assume a fixed relative humidity to derive the air humidity from the modeled air temperature. Seager et al. (1995a; SBK hereafter) introduced another model for the advective atmospheric mixed layer, which computes both the air humidity and temperature and hence determines its own relative humidity. The SBK model also avoids specifying the temperature above the modeled layer, which Kleeman and Power (1995) found necessary.

Here we will present simulations of the tropical oceans carried out with an ocean GCM coupled to the SBK atmospheric mixed-layer model. In addition to surface heat fluxes, ocean dynamics, and mixing processes are also important for determining SSTs. For ocean modelers, improving model physics is a challenge that has to be met by reproducing accurate SSTs and model dynamics given accurate surface fluxes. The ocean model we use is the reduced gravity, primitive equation ocean general circulation model of Gent and Cane (1989), with the embedded hybrid mixed-layer model of Chen et al. (1994a). This is the same ocean model as was used by Chen et al. (1994b) to examine the roles of vertical mixing, solar radiation, and wind stress on the seasonal cycle of SST in the tropical Pacific. We present not only the model SST simulations,

but also demonstrate that the seasonality of the model dynamics and thermodynamics compare well with other models and available observations. We believe that it is important to present SSTs and dynamics together for a model that computes heat fluxes without specifying atmospheric quantities over which the ocean has direct control. This is essential not only to demonstrate the model's ability to predict SSTs but also to test its suitability for coupling to atmospheric models. Ocean model experiments that pay careful attention to the surface heat flux, while avoiding constraining the model SST toward its observed value (e.g., SZC, Seager 1989; Seager and Blumenthal 1994; Blumenthal and Cane 1989; Sennechael et al. 1994; Chen et al. 1994b), are a more accurate way of identifying model errors, improving model physics, and selecting candidates for coupling. The series of experiments that follow will serve to identify those regions in all three tropical oceans where a local equilibrium approach to the surface heat flux is inappropriate.

In section 2 we describe the ocean GCM and the atmospheric mixed-layer model. The tropical Pacific, Atlantic, and the Indian Oceans are simulated individually with closed boundaries and the results are presented in section 3. In section 4 we discuss the general implications of our results to tropical ocean modeling, and section 5 contains the summary.

2. Model description

a. Ocean general circulation model

The ocean GCM employed for these studies is the reduced gravity, primitive equation model of Gent and Cane (1989), which was specifically designed for studying the interactions between the dynamics and thermodynamics of the upper tropical oceans. This model introduced an approach to efficiently achieving finer vertical resolution just below the mixed layer and in the thermocline region of high vertical shear. The vertical structure of the model ocean consists of a mixed layer and a specified number of layers below according to a sigma coordinate. The mixed layer depth and the thickness of the last sigma layer are computed prognostically and the remaining layers are computed diagnostically such that the ratio of each sigma layer to the total depth below the mixed layer is held to its prescribed value. The horizontal "A" grid (Arakawa and Lamb 1977) with local stretching is computationally efficient for resolving the regions of interest. Fourth-order central differences are employed in the horizontal with second-order central differences in the vertical. The Lorenz N-cycle scheme (Lorenz 1971) is used for time-integration and a high-order, scale-selective Shapiro Filter provides horizontal friction.

A hybrid vertical mixing scheme was developed and embedded in the Gent and Cane (1989) model by Chen et al. (1994a). The advantages of the traditional bulk mixed layer model of the Kraus–Turner (1967) type was combined with the dynamic instability model of Price et al. (1986) to simulate the three major processes of oceanic vertical turbulent mixing. The bulk mixed-layer model relates the atmospheric forcing to the mixed layer entrainment/detrainment; the gradient Richardson number mixing accounts for the shear flow instability; and an instantaneous adjustment simulates the high-frequency convection in the thermocline. Chen et al. (1994a) presented improved surface mixed-layer results both on and off the equator with this hybrid mixed-layer model. The Gent and Cane (1989) model with the hybrid mixed-layer model was combined with the SZC heat flux formulation by Chen et al. (1994b). The same ocean GCM is coupled to the atmospheric mixed-layer model of SBK here. As in the previous studies mentioned above, salinity effects are neglected in order to concentrate on the effects of surface heat flux parameterization on model SSTs and dynamics.

b. Atmospheric mixed-layer model

The atmospheric mixed-layer (AML) model has been described by SBK, and here we will provide only a summary of its characteristics. The model represents either a dry convective layer or the mixed layer that underlies shallow marine clouds (e.g., Augstein 1978). It does not represent the entire PBL, which would normally be taken to include the cloud layer itself. Within the mixed layer, the air temperature and air humidity are determined by a balance between surface fluxes, horizontal advection by imposed winds, entrainment from above the mixed layer, horizontal diffusion and, for temperature, radiative cooling. Closure assumptions are required to derive the entrainment. It is assumed, in common with many studies (e.g., Betts 1976; Nicholls and LeMone 1980), that the entrainment flux of virtual potential temperature is a fixed proportion of its surface flux. We also assume the humidity in the layer above the cloud layer is a fixed proportion of its mixed-layer value and that the mass entrainment is related to the generation of turbulence by friction at the surface. The last assumption is the most unconventional and is justified by its empirical success alone. With these assumptions, the air temperature and humidity, and hence the surface sensible and latent heat fluxes, can be calculated in terms of the ocean model SST and the imposed winds.

The results here indicate that atmospheric advection and eddy transports are capable of altering the relative humidity, and can be important in determining SSTs, even in the tropical Pacific. For midlatitude northern oceans lying east of continents in winter, dry, cold air flows out over warm waters. Surface fluxes are enhanced until the AML comes into equilibrium some distance offshore and this distance can be quite large. The AML model captures this process quite well during

northern winter over the Kuroshio and Gulf Stream (Seager et al. 1995a). In this work we will also show its importance for modeling tropical Atlantic and Indian Ocean SSTs.

To compute the longwave radiative heat loss from the surface we use a standard bulk formula and observed cloud cover (e.g., Seager and Blumenthal 1994). Solar radiative forcing is taken from the Earth Radiation Budget Experiment satellite data of Li and Leighton (1993). In summary, the complete heat flux can be computed with only the solar radiation, cloud cover, and winds needing to be specified. These are all quantities over which the ocean has only indirect control and can be justifiably externally specified. The quantities over which the ocean does have direct control, air temperature, and humidity, are modeled internally in terms of the SST, the winds, and their values at the continental margins.

3. Model results

The model domain for each of the oceans, horizontal and vertical resolutions, surface forcings, and initial and boundary conditions are listed in Table 1.

a. Model simulation of the tropical Pacific Ocean

The model is spun up from rest for six years and the results are presented for the two extreme months of the tropical Pacific seasonal cycle, namely, for March and September.

1) Model ocean circulation

Surface currents for the months of March and September are shown in Fig. 1. The South Equatorial Current (SEC) accelerates downstream with maximum speeds of over 100 cm s^{-1} at 160°W in September (adjacent grid points are averaged in vector plots). This is weaker than observed (Wyrtki and Kilonsky 1984) due to averaging over the mixed layer depth. The model SEC is stronger than other model results with comparable resolution (e.g., Philander et al. 1987) probably due to lower dissipation provided by the Shapiro filter. In Fig. 2 we show a Hovmoller diagram of the zonal current at 112°W. The spring reversal of the SEC (see Fig. 2) is too strong in the model and is caused by too much upwelling (which we will discuss later). The seasonal migration of the North Equatorial Counter Current (NECC) and the double core of the SEC, with maximum speeds occurring in fall in the Northern Hemisphere fall, agree well with observations (Reverdin et al. 1994; Halpern 1987).

The Equatorial Undercurrent (EUC) and a zonal section of model temperatures along the equator are shown in Fig. 3 for March and September. The model EUC,

Table 1. Model domain, resolution, and initial boundary conditions for the Pacific, Atlantic, and the Indian Ocean basins.

Domain:	
Pacific	124° E–284°E × 30°S–30°N
Atlantic	90°W–14°E × 40°S–30°N
Indian	32°E–126°E × 32°S–24°N
Horizontal resolution:	
Pacific	Longitude: 1°, stretched (1°/3) at the eastern and western boundaries Latitude: 2°/3, stretched (1°/3) within 10°S–10°N
Atlantic	Longitude: 1°/2 stretched (1°/3) in the Gulf Stream region and the eastern boundary Latitude: 2°/3, stretched (1°/3) within 3°S–3°N
Indian	Uniform 1°/2 × 1°/2
Vertical resolution:	
Pacific	Hybrid mixed layer + 11 σ-layers with σ = 0.0286, 0.0286, 0.0286, 0.0429, 0.0429, 0.0429, 0.0714, 0.1429, 0.1429, 0.1429, and 0.286
Atlantic	Hybrid mixed layer + 14 σ-layers with σ = 0.0286, 0.0286, 0.0286, 0.0286, 0.0429, 0.0429, 0.0429, 0.0429, 0.0714, 0.0714, 0.0714, 0.0714, 0.1429, and 0.286
Indian	Hybrid mixed layer + 14 σ-layers with σ = 0.0286, 0.0286, 0.0286, 0.0286, 0.0429, 0.0429, 0.0429, 0.0429, 0.0714, 0.0714, 0.0714, 0.0714, 0.1429, and 0.286
Wind stresses	
Pacific	FSU winds with $C_d = 1.5 \times 10^{-3}$
Atlantic	Hellerman and Rosenstein (1983)
Indian	Hellerman and Rosenstein (1983)
Initial conditions:	Initial Stratification derived from Levitus (1982)
Boundary conditions:	No slip and no heat flux conditions at lateral boundaries. Relaxation to Levitus (1982) climatology: Pacific: over 20°–30°S and 20°–30°N Atlantic: over 30°–40°S and at 30°N Indian Ocean: over 22°–32°S
Mixed-layer constants:	Wind-mixing coefficient, m = 1.25 Buoyancy coefficient, n = 0.83

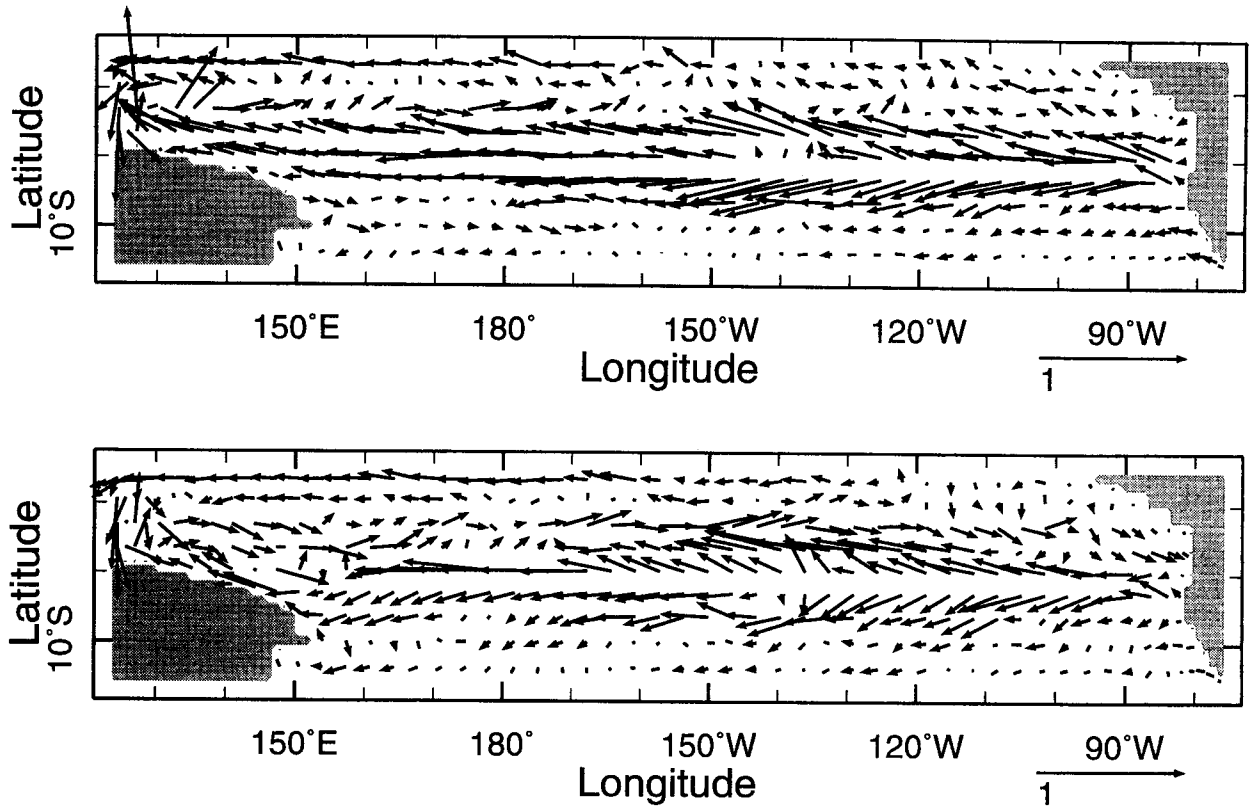

FIG. 1. Monthly mean surface currents for March and September (m s^{-1}). Note the South Equatorial Counter Current in March at about 8°S in the west and the strong North Equatorial Counter Current in September.

with core speeds of over 160 cm s^{-1}, is similar to other models (e.g., Philander et al. 1987). However, it is stronger than observations (McPhaden and McCarty 1992) with a strong reversal of the SEC in April. The drag coefficient used in creating the wind stresses was not tuned and may be partly responsible for both these model failings.

The temperature section along the equator shows a fairly strong thermocline with an east–west slope of over 150 m for the 20°C isotherm. Stronger wind stresses, mentioned above, are also responsible for stronger surface currents and a larger slope for the thermocline than observed. The seasonality of equatorial troughs, ridges, and the shoaling at 10°N of the model thermocline (seen in the meridional section; not shown) are qualitatively similar to observations (Wyrtki and Kilonsky 1984) and compare well with other model results (Murtugudde et al. 1995; Stockdale et al. 1993). Doming near 10°N (not shown) is better simulated than Gordon and Corry (1991), albeit weaker than observed. Probable causes for the lack of doming are the same as pointed out by Gordon and Corry (1991), that is, errors in wind stress curl and lack of horizontal and vertical resolution in the NECC area.

2) MODEL SST SIMULATION

Model SSTs are compared to Levitus data and the differences are presented for March and September in Fig. 4. The model displays a bias in some regions and has seasonally varying SST errors in others. Around the dateline, model SSTs are warmer than observed for both months reaching a maximum of about 1°C in March. Between 150° and 120°W, the model has a cold bias of up to 1°C. Further to the east, from 120°W to the coastline of South America, the model has seasonally varying SST errors. These errors are less than 1° to 2°C everywhere except in a very narrow region at the southern tip of South America.

The warm bias around the date line is related to the shallow mixed-layer depths (MLDs) in this region. The MLD here is typically about 40–50 m deep. In the hybrid mixed-layer model the MLDs in regions of low current shear are mainly determined by TKE generation and the buoyancy forcing. As pointed out by Oberhuber (1993), the low TKE generation by wind stresses in the western equatorial Pacific results in shallowing of the mixed layer (also see Fig. 2 of Chen et al. 1994b). Since the annual mean net flux is downward in this region, the net heating of a shallower than observed

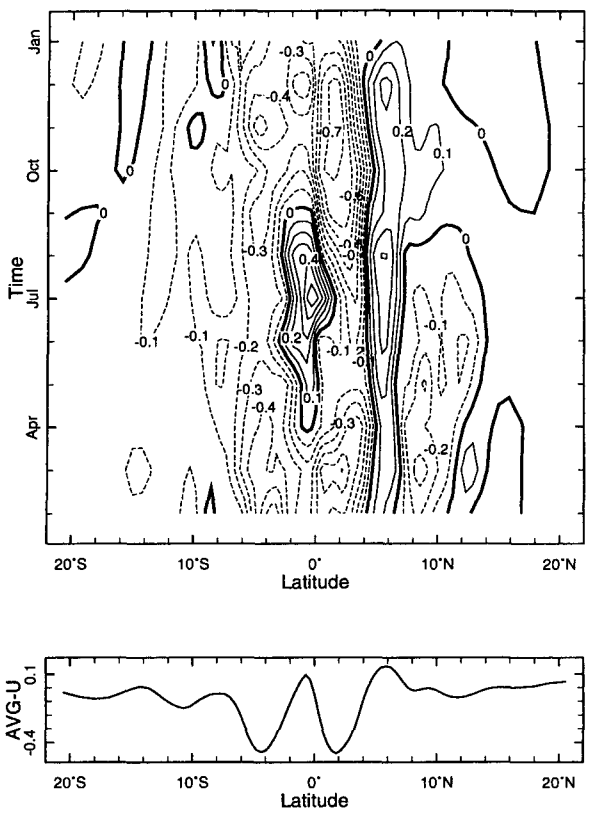

FIG. 2. Seasonal cycle of the zonal current along 112°W (contour interval 0.1 m s^{-1}) and a meridional section of annual mean zonal velocity. Note the double maxima in SEC and the relatively low seasonal variability to the south of 4°S.

mixed layer results in warmer than observed SSTs. Seager and Blumenthal (1994) used a constant MLD of 50 m and obtained SSTs that are warmer than observed. Our SSTs are warmer still because, in their case, MLDs are maintained by entraining cold waters from below, whereas in the present model the ML can shallow due to horizontal divergence without entrainment. Moreover, in the hybrid ML model, warmer SSTs lead to further shallowing of the mixed layer by increasing the temperature jump at the bottom of the mixed layer. Lack of salinity and the freshwater forcing in the model is a shortcoming for resolving the mixed-layer processes in this region (Shinoda and Lukas 1995).

To alleviate the cold bias in the upwelling region between 160° and 120°W, the wind stresses were reduced by 20% in a separate experiment and the model was run for 2 years. The weaker wind stresses resulted in a considerable reduction in the area with a cold bias and reduced the errors by 0.5°–1°C. However, it also lead to a warming near the dateline for two reasons: an even shallower mixed layer due to reduced TKE generation and less westward advection of cold water. While a uniform reduction of the drag coefficient will improve the SSTs in areas of upwelling, it will have adverse effects elsewhere.

The wind-mixing term in the Kraus–Turner model is decided by an empirical constant (see Table 1) that is often used as a tuning coefficient. Our experiment with doubling the parameter (which acts to increase the MLDs for the same wind stress) resulted in the following: in the eastern equatorial Pacific, where the net heat flux is into the ocean, deeper MLDs lead to cooling of the already colder than observed SSTs in April; at higher latitudes where the net flux is outward, the model gets warmer in a region of already warmer SSTs. Increasing the penetrative solar radiation has effects similar to increasing the TKE generation term; that is, SSTs get colder in the regions of cold bias. Thus, only the western equatorial Pacific improves due to increased MLDs. It is evident that the parameter for TKE generation will have to be made spatially dependent (e.g., Chang 1994; Wang et al. 1995) to achieve better wind-mixing effects on MLDs.

In the eastern equatorial Pacific, close to the coast of South America, the model has colder than observed SSTs in March and warmer than observed SSTs in September. A heat budget calculation for 110°–80°W and 10°S to the equator is shown in Fig. 5 along with the seasonal variation of SST errors along the equator. The SST errors show no westward propagation indicating that the seasonal cycle is modeled correctly although the model displays errors in amplitudes. In March/April, the heat loss due to zonal advection and cooling due to upwelling are at their peak due to shallow MLDs (weak winds). Net flux is downward throughout the year with a prominent annual cycle with a lower peak in fall due to low clouds over cold SSTs during that time. Annual mean corrective fluxes in this region are nearly 100 W m^{-2}, which is larger than the uncertainties in solar radiative forcing (Chen et al. 1994b; Seager and Blumenthal 1994). The model also fails to produce a strong eastern boundary current along the coast (see Fig. 1), which may further impact the poor simulation of the SST variability in the cold tongue.

In contrast, cold biases of 1°C or less in the western boundary current regions in both hemispheres and to the north and south of the equator in the east can be corrected by fluxes of the order of 25°W m^2. Corrective fluxes of this size are at the margin of the probable errors in solar radiation, making it difficult to identify model errors.

To assess the effects of diffusion and advection of atmospheric moisture, the model was run for 4 years with the atmospheric mixed layer turned off. The average relative humidity of the run with atmospheric advection and diffusion was used. This surface heat flux parameterization is then similar to that of Seager and Blumenthal (1994). The differences between model SSTs from this run and Levitus (1982) data (Fig. 6) are clearly larger than those when the AML model is employed (Fig. 4). Model SSTs are warmer in the cold

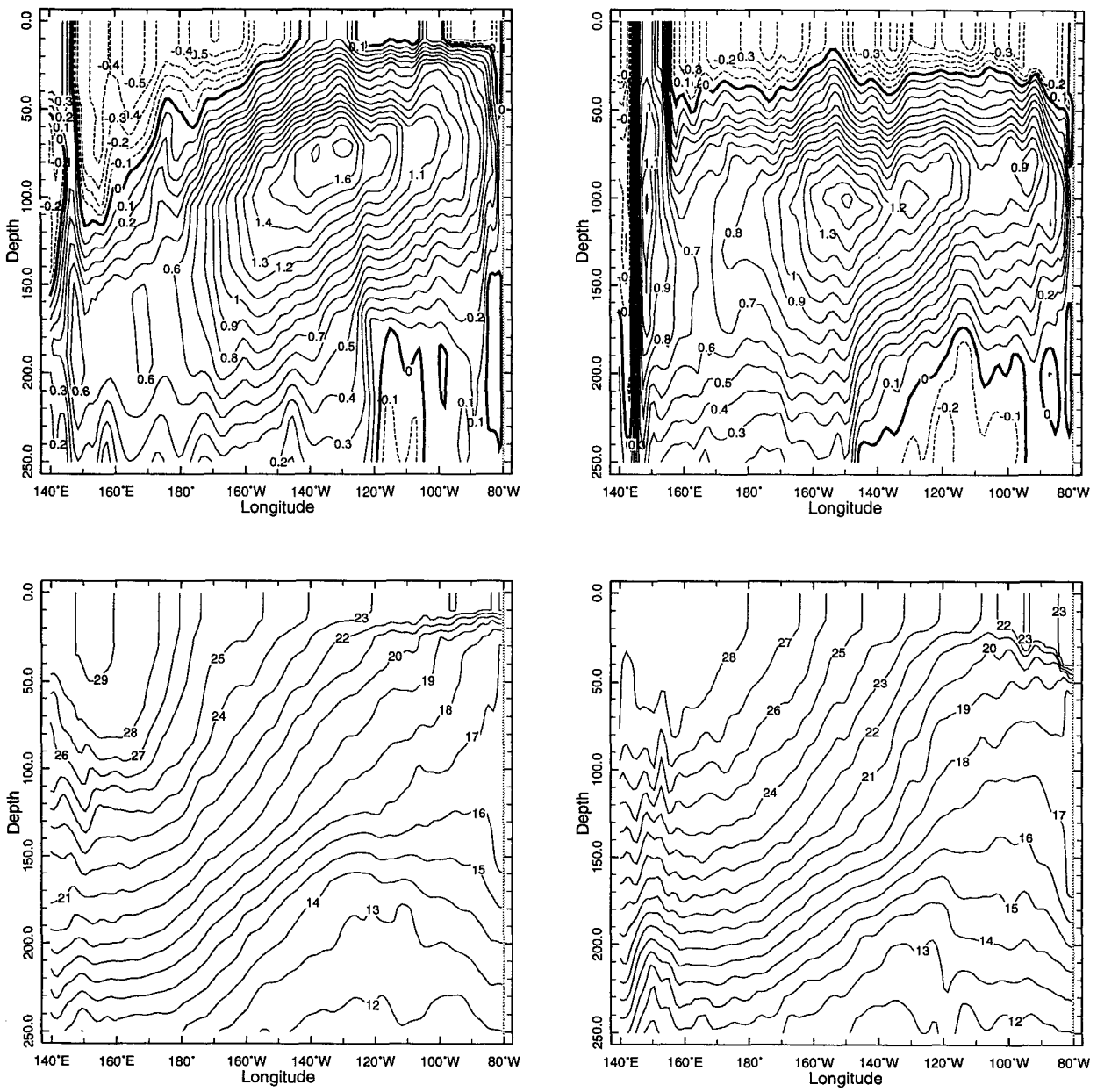

FIG. 3. The Equatorial Undercurrent (contour interval 0.1 m s^{-1}) and the model thermocline along the equator for March and September. The model reproduces a strong EUC and the east–west slope of the thermocline.

tongue region with the AML because the diffusion results in a local maxima in relative humidity and lower latent heat fluxes. Advection of cooler, drier air equatorward leads to cooler SSTs in the east when the AML is used. Along 15°S and 15°N, the model SSTs are also cooler when the AML is used because of equatorward advection of moisture. In these regions of nearly one-dimensional heat balance, a slight warming of the ML can be amplified by the positive feedback due to stabilization of the ML. It is evident that even in the tropical Pacific, the assumption of a constant relative humidity, that is the assumption that the AML is in local equilibrium with the underlying ocean, is not quite right.

b. Model circulation of the tropical Atlantic

Initial experiments with 9 and 12 layers for the tropical Atlantic resulted in a very weak model thermocline. The results are presented here for a model sim-

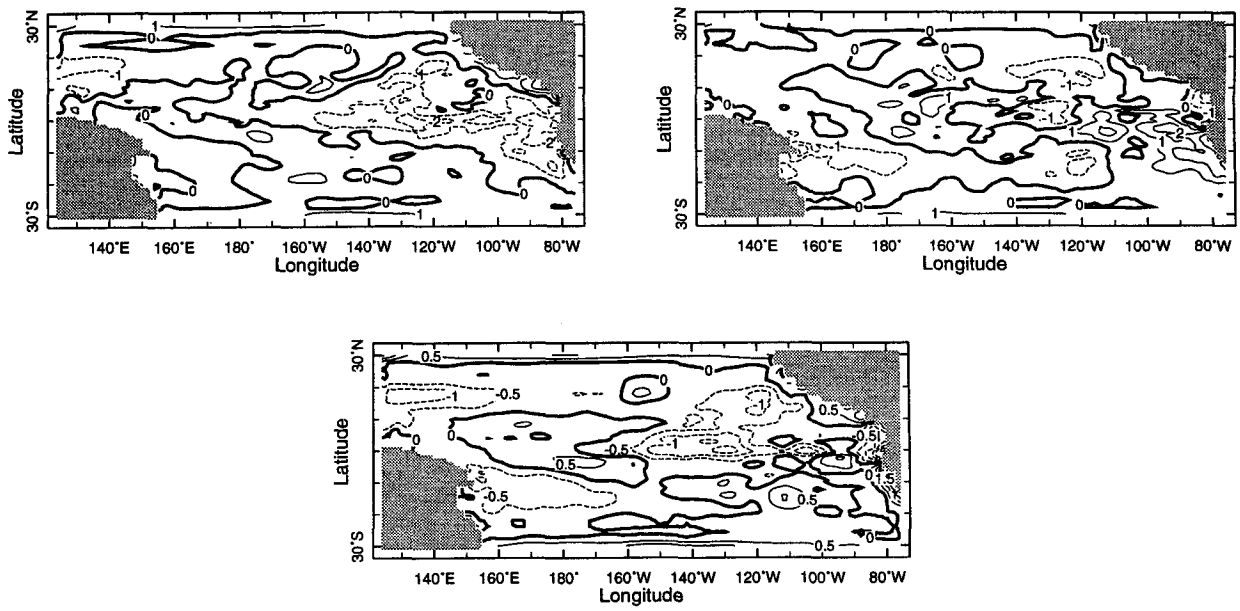

FIG. 4. Model SSTs with AML: top panels show the differences between model SSTs and Levitus data for March (left) and September (right)(contour interval 1°C). The bottom panel shows the differences in annual mean model and Levitus SSTs (contour interval 0.5°C).

ulation with 15 layers in the vertical for year 8 of the spin up from rest. Note that (see Table 1) the resolution just below the mixed layer is higher than that for the tropical Pacific grid. In the Northern Hemisphere, since the effects of the advection of dry air off the African continent on SSTs is of special interest, relaxation to Levitus climatology was enforced only at 30°N (see Table 1). Model results are presented for the two extreme months of the seasonal cycle, namely, for March and September.

1) MODEL OCEAN CIRCULATION

Surface currents for March and September are shown in Fig. 7. The seasonal dependence of the currents generally agrees well with the historical ship drift data of Richardson and McKee (1989). Spurious eastward currents west of 20°W in March are probably caused by the overestimation of the wind stress curl (Hellerman and Rosenstein 1983). Maximum speeds of over 115 cm s^{-1} occur in the North Brazil current in September and maximum current speeds in the NECC reach over 120 cm s^{-1}. The NECC continues as the Guinea Current into the Gulf of Guinea. The seasonality of the surface currents in the Tropics is in good agreement with other model results (e.g., Oberhuber 1993; Philander and Pacanowski 1986; Sarmiento 1986). The Caribbean and Florida Current in Fig. 7 are weaker than observations and weak eastward currents occur along the northern coast of South America. In these regions, the absence of bottom topography and the modified geometry (no islands) of the passage are likely sources of error in addition to uncertainties in the wind forcing.

The EUC (Fig. 8) has maximum core velocity of about 90 cm s^{-1} in March and is slightly weaker than observations (Philander 1973; Wacongne 1988, 1989). The EUC is closer to the surface in the west during the Northern Hemisphere spring, while it has a significant east–west slope during the fall. Spurious eastward surface currents mentioned above are also seen in Figs. 8 and 9 to the west of 30°W during the NH spring. As seen in Fig. 9, there is a semiannual harmonic in the east in zonal surface currents, which is a local response to the winds (Philander and Pacanowski 1987). The westward propagating instability waves that are seen between June and October correspond to the strengthening of the southeast winds. The local eastward winds in the Gulf of Guinea are also responsible for the downward slope of the isotherms in the east in September. The east–west slope of the 20°C isotherm is minimum in March/April and about 100 m in September. Despite the stronger southeasterly winds in September, the thermocline shoals in the east (vertical movement of the 20°C isotherm is about 50 m) due to a remote response to the winds in the west (Philander and Pacanowski 1987). A meridional section of temperature versus depth (not shown) also shows the trough under the NECC at about 3°N and the ridge at 10°N indicating the geostrophic balance of the NECC.

2) MODEL SST SIMULATION

Differences between model SSTs and Levitus data are presented in Fig. 10. Seasonal variations of SST

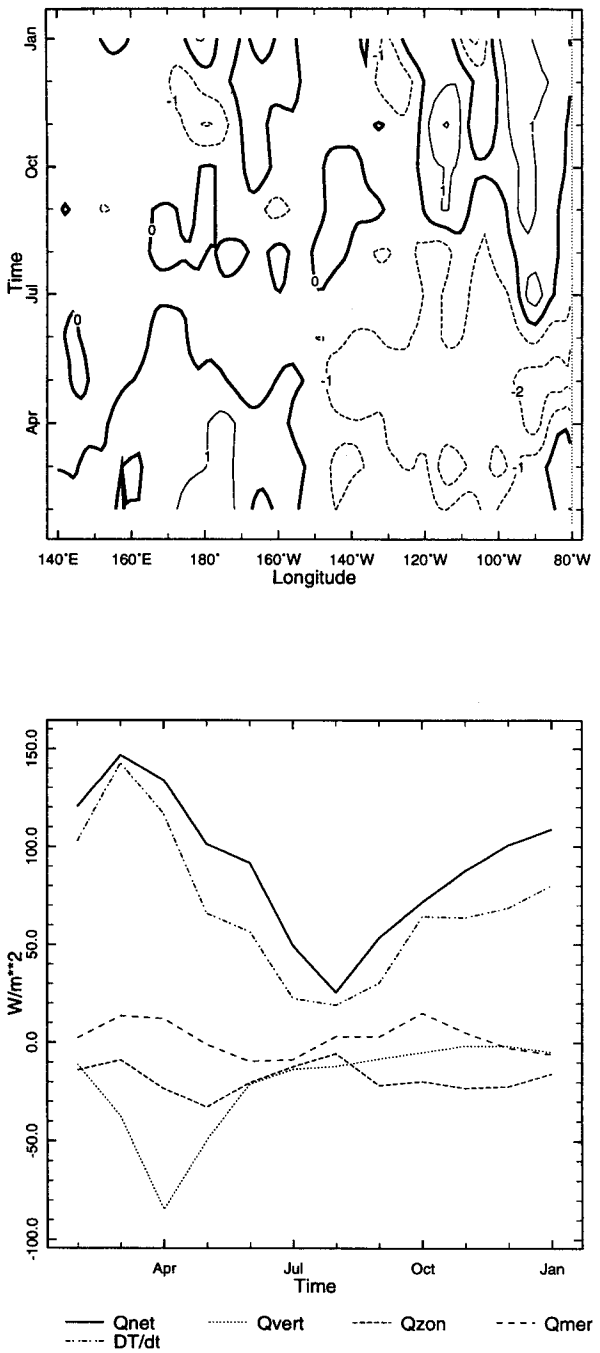

FIG. 5. Seasonal variations of SST errors along the equator (top; contour interval 1°C) and the heat budget for the mixed layer in the east (integrated over 110°W–80°W and 10°S to the equator).

errors in the eastern equatorial Atlantic are similar to the error patterns in the Pacific (Fig. 4). Model SSTs are too cool in March and too warm in September. To the south, warm biases persist of up to 3°C at the southern tip of the African continent and over 1°C in the region of the Brazil Current. Model SSTs are colder than observed by up to 3°C in the Gulf of Mexico region where the model fails to produce strong northward transport of warm equatorial waters (note the weak western boundary current in Fig. 7).

Seasonal variation of SST errors along the equator (Fig. 11) show an annual cycle in the east with colder than observed SSTs in the early part of the year and warmer SSTs during the Northern Hemisphere summer and fall. The heat budget for the eastern equatorial Atlantic is shown in Fig. 12. The net surface flux is downward throughout the year with the maximum in April and the minimum in December. The surface heat flux dominates the heat budget until April. However, cooling due to meridional advection and upwelling increase from May until July. The net effect seems to be excess cooling of model SSTs. As the trade winds get stronger from May onward, warming due to zonal advection gets stronger until July but weakens as the zonal SST gradient drops from July onward. The strengthening SECC (see the reversal of meridional currents in the east at 10°S in Fig. 7) reverses the contribution of meridional advection from cooling to weak warming after October. In combination with a reduced cooling due to upwelling, warmer than observed SSTs form in July and persist through October. In the area along 25°S where large SST errors are found the heat budgets are almost identical (not shown). Both the region off Africa and the area further west are dominated by the net surface heat flux. This displays an annual cycle with heat loss from April through October and gain from November to March. The upwelling and advection terms are negligibly small. Off Africa the errors may be related to the weak eastern boundary current in this region. However, it is probable that the ML physics simply does not reproduce realistic seasonal variations. Lack of observations in these regions makes it difficult to identify model deficiencies.

The effects of atmospheric advection and diffusion of air humidity are seen in Fig. 13, where the differences in model SSTs with the local equilibrium mixed-layer model and Levitus (1982) data are shown. Model SST errors are twice as large when compared to the errors when the AML model is used (Fig. 10). Note that the largest errors occur in the same region for both cases (along 25°S) pointing to an amplification of SST errors due to positive feedback between mixed-layer physics and the surface heat fluxes. Advection of dry air off the African (winter) continent in March results in colder SSTs when the AML is used for computing surface heat fluxes. As in the Pacific, diffusion of air humidity leads to a local maximum in relative humidity in the AML, and thus warmer SSTs, over the equatorial Atlantic. In the Southern Hemisphere, the region around 20°W and 25°S, where the model was warmer than observed when coupled to the AML (Fig. 10), gets even warmer when a local equilibrium mixed layer is assumed. These results affirm the importance of atmospheric transports in determining the fluxes and SST

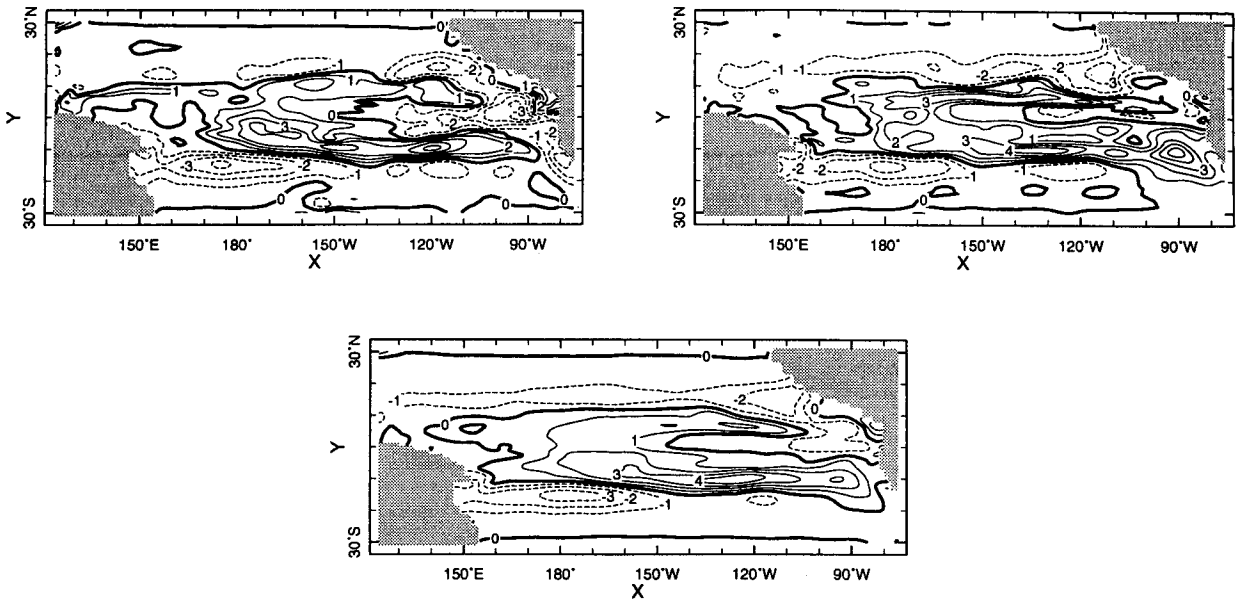

FIG. 6. Differences between model SSTs with a local-equilibrium heat flux and Levitus data (contour interval 1°C): for March (top left) and September (top right) and the annual mean differences (bottom).

over the entire tropical Atlantic. More importantly, model dynamics is affected by inaccuracies in surface heat fluxes, which are masked by flux-restoring type parameterizations (Haney 1971).

c. *Model simulation of the Indian Ocean*

The model is spun up from rest with Hellerman and Rosenstein (1983) climatological winds. The results

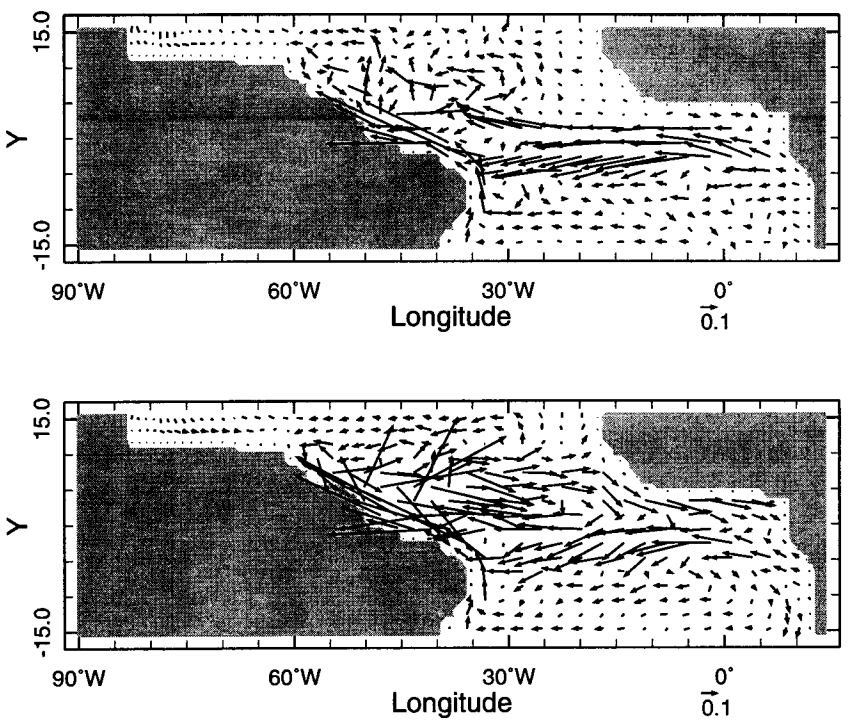

FIG. 7. Surface currents (m s^{-1}) for March and September. Seasonality of the equatorial currents is reasonably reproduced with a strong NECC in September that penetrates to the coast.

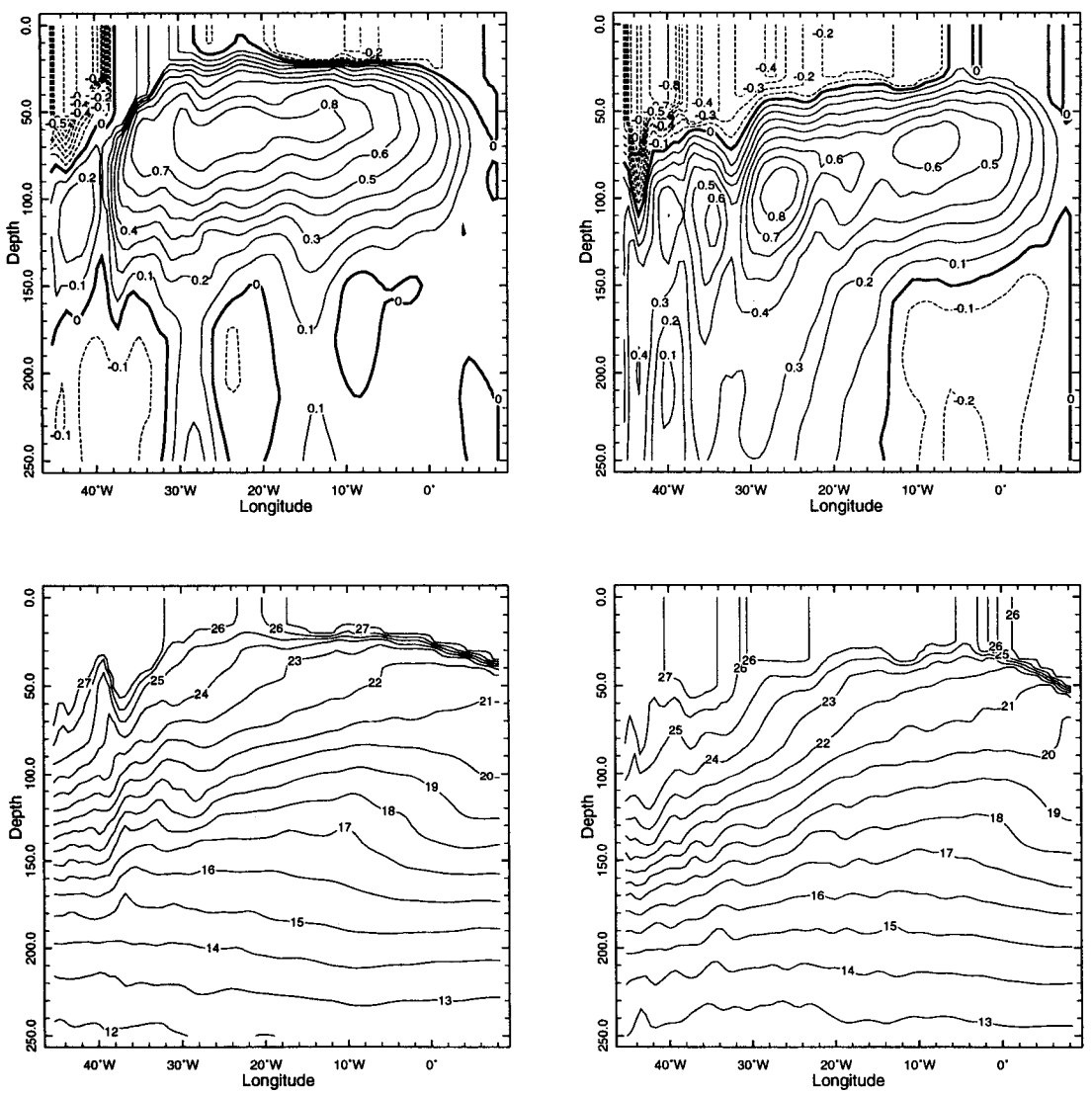

FIG. 8. Equatorial Undercurrent (contour interval 0.1 m s^{-1}) and a temperature section along the equator in March and September. Seasonality of the EUC and the model thermocline agree well with observations.

are presented for February and August (extremes of the winter and summer monsoons) of year 8.

1) MODEL OCEAN CIRCULATION

Surface currents are shown in Fig. 14 for February and August. The seasonal reversal of the Somali Current from February to August is clearly seen in the model results with peak speeds of over 180 cm s^{-1} in August. As in McCreary et al. (1993), the speeds in the Somali Current are larger than average speeds obtained from ship drift and buoy data (Richardson and McKee 1989; Molinari et al. 1990), but lower than the synoptic cruises (McCreary and Kundu 1988). The complex structure of the Somali Current with the onshore and offshore currents are reasonably reproduced including the Great Whirl centered around 9°N. The simulations of McCreary et al. (1993) failed to develop the Great Whirl, and they did not explain the reasons for this failure. The present model differs from their model in horizontal and vertical resolutions, horizontal friction, and more importantly in the representation of mixed-layer processes and its interaction with the thermocline. The SECC, which is fed by the southward Somali Current in February, reaches over 50 cm s^{-1} in the west. The structure of the SECC is in close agreement with the historical ship drift data of Richardson and McKee (1989), and the model results of McCreary et al. (1993) and Woodberry et al. (1989).

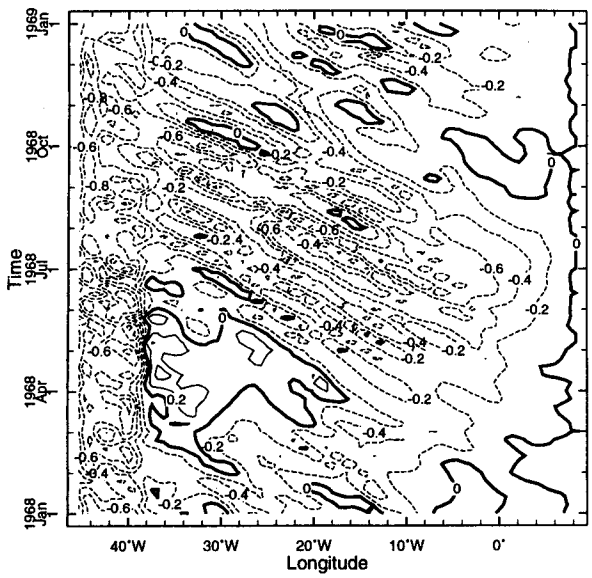

FIG. 9. Seasonal cycle of the zonal currents along the equator (contour interval 0.2 m s^{-1}). Note the semiannual cycle in the east and the annual cycle in the west. Increased instability wave activity from June onward corresponds to increased southwest winds.

The seasonality of the SEC is in close agreement with the ship drift climatology of Cutler and Swallow (1984). The wind-driven eastward jet near the equator (Wyrtki 1973) is reproduced in the model during transition periods of the monsoons (not shown) and has speeds of over 1 m s^{-1} in May. The current speeds and the meridional extent and weakening of the jet in August all agree with Richardson and McKee (1989). The model also produces a strong Equatorial Jet ($\sim$140 cm s^{-1}) in November (Reverdin et al. 1983), which is clearly absent in McCreary et al. (1993). The NEC in February (Fig. 14) occupies the region between the equator and 10°N with maximum current speeds of about 80 cm s^{-1}. The flow direction in the Bay of Bengal and to the south of Sri Lanka have fully reversed in August compared to the circulation in February.

The complex seasonal variability of the winds not only affects the surface currents but also the vertical structure of the currents. An EUC with westward surface currents and eastward subsurface currents exists from January to March in the western Indian Ocean (Swallow 1967; Knox 1976). The surface flow reverses by April and the subsurface flow has a semiannual variation (Luyten and Roemmich 1982). Model results reproduce the reversal of the surface and subsurface flows as shown in Fig. 15 with core velocities that are comparable to observations. The role played by the waves in subthermocline adjustments is addressed by Jensen (1993).

A meridional section (60°E) of temperature is shown in Fig. 16 for August and November. Reverdin and Fieux (1987) note a pinch in the thermocline north of 8°S and the model reproduces the corresponding ridge in August. The downwelling to the south of the ridge associated with the SEC leads to the deepening isotherms centered at about 20°S, which is similar to Levitus (1982). The changes in the model thermocline structure during the SW monsoon are in good agreement with the observations. The deep thermocline centered at 8°N is associated with the anticyclonic Great Whirl. The depth of the 20°C isotherm shows the largest variability north of 5°N, in qualitative agreement with Fig. 4 of Reverdin and Fieux (1987).

2) MODEL SST SIMULATION

The differences between model SSTs and Levitus data are shown in Fig. 17. In February, the model is colder than observed by about 2°C near 20°S and 85°E and also off the west coast of India. Both these regions have a cold bias of about 1°C, which also shows up in the annual mean SST differences. Model SSTs are warmer in the Somali current region for both months shown here with a warm bias of about 1°C in the annual mean. McCreary et al. (1993) obtained SST errors that are slightly smaller. Note, however, that they specify air temperature and air humidity from observations.

Net surface flux is downward in February in the entire domain except at the northern border at 65°E. Seasonal variations of model MLDs are comparable to those derived from observations of thermal structure by Rao et al. (1989), and the corrective fluxes are in the range of 25 W m^2 over the whole domain. Standard deviations of the model SST compare very well with Levitus data. It is, thus, evident that model SST errors can be eliminated by heat fluxes that are well within the errors in solar radiative forcing (Seager and Blumenthal 1994; Chen et al. 1994b).

Differences in model SSTs with the local equilibrium mixed-layer model and Levitus (1982) are significantly larger (Fig. 18) compared to SST errors with complete AML (Fig. 17). During the boreal winter, advection of dry air off continents by northeasterly monsoons result in locally low relative humidities off the west coast of Burma and India. Easterlies carry dry air off the Australian continent during both seasons, although they are much stronger during the boreal summer. The local maxima in relative humidities off the east coast of Africa are generated by atmospheric diffusion. This is especially so during August when the strong northward Somali Current generates cold coastal SSTs due to upwelling. The basin average relative humidity from the run with the AML is higher than the modeled relative humidity off Australia and lower off Somalia and off the east coast of India. When this basin mean relative humidity is used in the local equilibrium mixed-layer scheme, the model SSTs become warmer off the coast of Australia and colder off the coasts of Somalia and eastern India. The positive feedback between the SSTs and the ML are again seen as slightly deeper MLDs in the regions of colder SSTs.

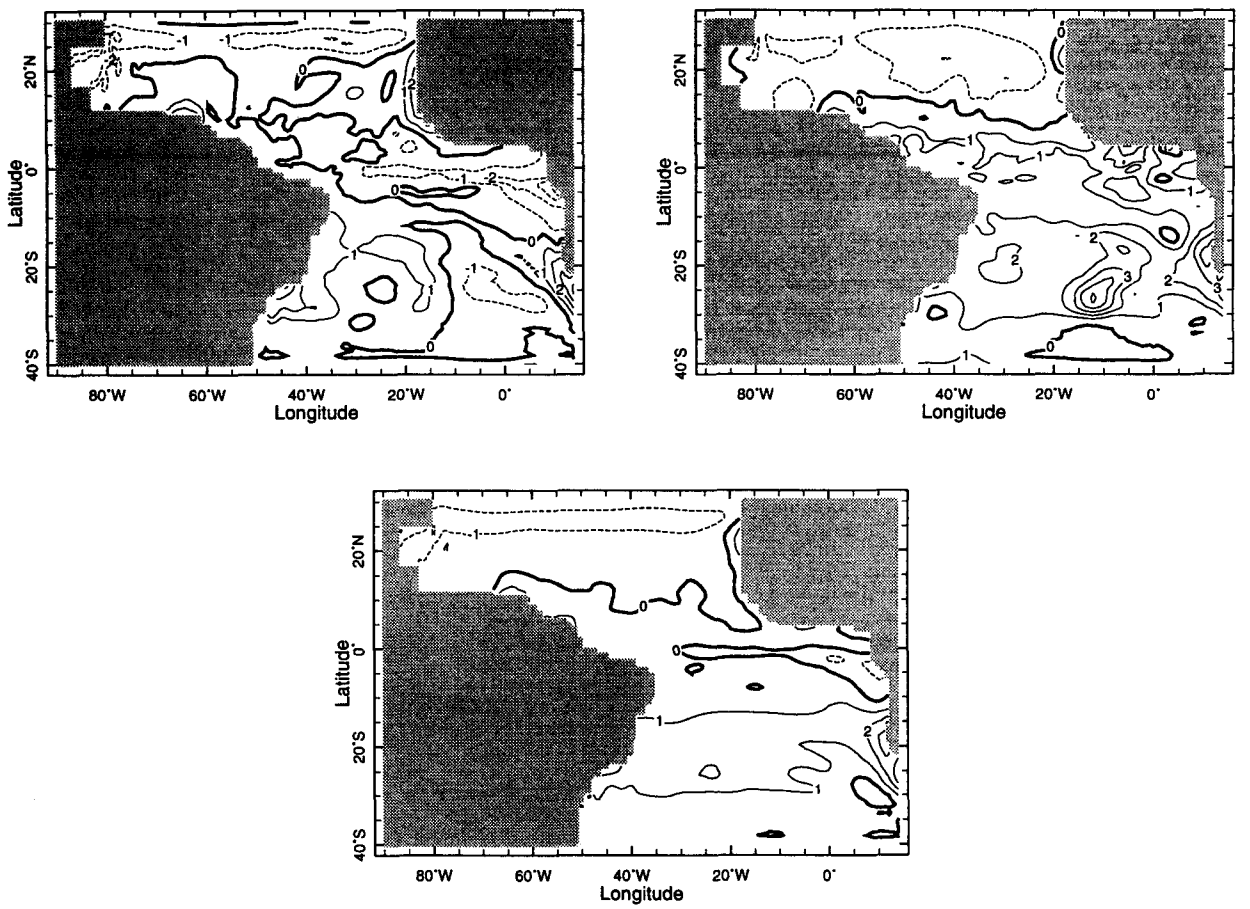

FIG. 10. Model SSTs with AML: Top panels show the differences between model SSTs and Levitus data (contour interval 1°C) for March (left) and September (right). The bottom panel shows the differences in annual mean model and Levitus SSTs.

4. General implications for tropical ocean modeling

A major motivation for the development of this ocean GCM was the need to overcome perceived inadequacies of linear dynamical ocean models with simplified thermodynamics. These had demonstrated considerable skill at predicting tropical Pacific SST (SZC) but were thought to be inadequate for the task of modeling tropical Atlantic SST. Indeed, Blumenthal and Cane (1989), using an optimization technique that found the model parameters that gave the most realistic SST simulation, concluded unambiguously that the model of SZC was inappropriate for simulating Atlantic SST. Sennechael et al. (1994), using a similar method of model tuning, and the same ocean model came to the same conclusions. In both cases their SST errors were enormous, reaching up to 5°C off the African coast during Northern Hemisphere spring. A somewhat surprising result of the work presented here is that nonlocal equilibrium heat flux formulation is, by far, the most important. Coupling the GCM to an atmospheric mixed layer that is in local equilibrium with the underlying SST, as was done in these earlier studies, led to SST errors comparable to those of Blumenthal and Cane (1989) and Sennechael et al. (1994). When advection and diffusion are allowed to influence the atmospheric humidity and temperature, these errors are almost entirely removed. Indeed, the SST errors are reduced not just off the coast of Africa but also in the western portions of the ocean. Obviously this is compelling evidence that, for this ocean at least, the effects of atmospheric transports of heat and moisture need to be properly accounted for in the heat flux formulation.

The arguments for using the kind of heat flux boundary condition employed here rest on the observation that the lowest layer of the atmosphere adjusts to the underlying SST (Betts and Ridgway 1989) such that using observed atmospheric quantities in the heat flux computation is predisposing much of the answer. Is this argument then in contradiction to our demonstration of a distinctly nonlocal relationship between the marine boundary layer and the SST? It is not because what is occurring in nature is a coupled interaction between the

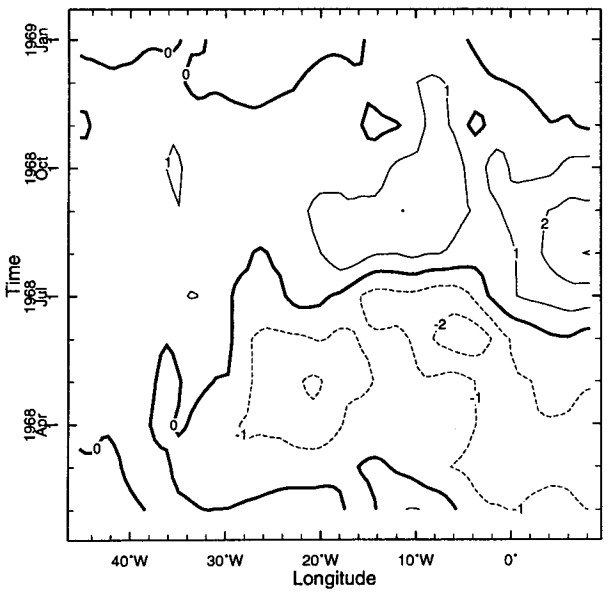

FIG. 11. Seasonality of SST errors along the equator (contour interval 1°C). Model SSTs depart from observed SSTs mostly to the east of 30°W.

ocean and the marine boundary layer. Consider the case of winds flowing from the coast of Africa and westward over the subtropical Atlantic. These winds advect dry air from cooler waters to the north and from off the African coast. As they flow west the dry air moves over warm waters and leads to a large flux of moisture from the ocean into the atmosphere. For the case of a fixed SST and fixed advecting wind, we can calculate the distance over which the boundary layer equilibrates. For an atmospheric mixed layer with pressure thickness P, advecting wind U flowing in direction r over an SST with saturation humidity q_0, and ignoring diffusion, the air specific humidity, q, is given by

$$PU\frac{dq}{dr} = C_0\omega_0(q_0 - q) - C_0\omega_0\mu q, \qquad (1)$$

where C_0 is the surface exchange coefficient and ω_0 is a surface velocity scale related to U by $\omega_0 = UP/h$ with h the depth of the mixed layer. The last term on the right is a parameterization of entrainment at the mixed-layer top (see SBK). This has the solution

$$q(r) = q(r_0)e^{-a\Delta r} + \frac{q_0}{1+\mu}(1 - e^{-a\Delta r}), \qquad (2)$$

where $q(r_0)$ is the upstream value and Δr is the distance traveled and μ is an adjustable parameter that approximates relative humidity to be 80% for local equilibrium (see Seager et al. 1995). The e-folding distance, a, is $h/C_0(1 + \mu)$ and for typical values is on the order of 400 km. This draws attention to the quite short distance needed for boundary layer adjustment to the underlying SST.

However, the situation is not quite this simple. In reality, the enhanced moisture flux into the dry advecting air cools the SST, which reduces the boundary layer equilibrium value and the moisture flux. The coupled interaction has the effect of propagating the influence of the advecting dry air downstream. Furthermore, the cooled SSTs are advected westward by the ocean currents. The net effect is that the influence of dry advecting air can extend over considerably more of the Atlantic Ocean than simple adjustment of the boundary layer to an unvarying SST would suggest.

The latent heat fluxes off West Africa in the two simulations are actually quite similar even though the case with the complete AML model has much lower SSTs. This observation is *not* an indication that advection of dry air in the atmosphere is unimportant. It is instead an indication of the degree of coupling between the fluxes and the SST with both being reduced as the nonlocal equilibrium is established. The tight coupling, and the dependence of model SST upon it, is a very clear indication of the need to accurately model the feedbacks between fluxes and SST.

It is worth considering what this implies for the heat flux boundary conditions used in earlier work. Sennechael et al. (1994) assumed a fixed relative humidity of about 73% in a local equilibrium heat flux model. Blanke and Delecluse (1993) also assumed a fixed relative humidity but imposed the observed air temperature. This forced the air humidity to be reasonably close to its observed value. It is hardly surprising that their SST errors were hence less than those of Sennechael et al. (1994), but this result is gained at the expense of

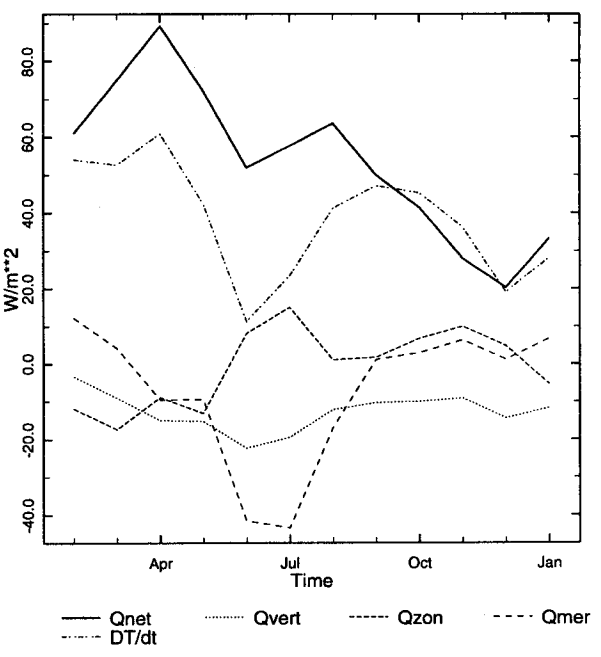

FIG. 12. Heat budget: averaged over 10°W–8°E and 5°S–3°N.

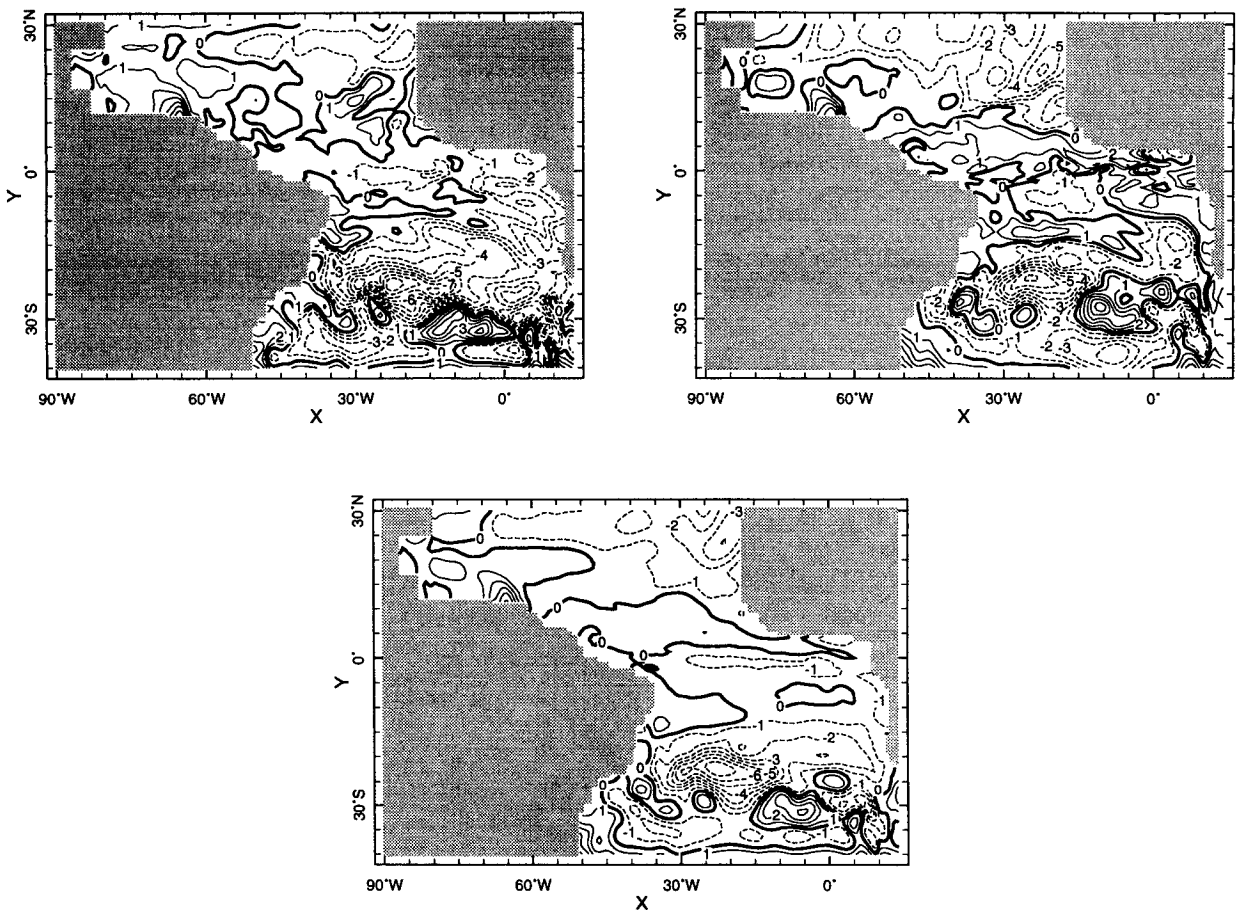

FIG. 13. Differences between model SSTs with a local-equilibrium heat flux and Levitus data (contour interval 1°C): for March (top left) and September (top right) and the annual mean differences (bottom).

distorting the SST–flux relationship demonstrated here. Their scheme is close to a relaxation type boundary condition. The analysis product of the European Centre for Medium-Range Weather Forecasts shows that the relative humidity minimum in April off West Africa is quite weak with values of about 72% surrounded by values closer to 80% (not shown). This is quite similar to the relative humidity computed by our coupled OGCM–AML model. If we were to stop thinking at this point, we might conclude that assuming a fixed relative humidity in the heat flux calculation might not be a bad approximation. However, this is not the case, since to do so is to remove knowledge of the upstream sources of drier and cooler air. The coupled ocean–marine boundary layer system may equilibrate at fairly high values of the relative humidity but it only does so through an interaction that lowers the SST. Merely assuming a fixed relative humidity and a local equilibrium will give SSTs that are too warm.

The importance of advection over the Atlantic was expected, but it is surprising that the SST simulation over the tropical Pacific is also notably superior in the case with the complete AML model. In other work (Seager and Blumenthal 1994, SBK) it had been argued that the large size of the Pacific Ocean made the local equilibrium assumption of the earlier heat flux schemes appropriate. Instead it is apparent that a nonlocal scheme can lead to discernible improvements in the SST simulation. The complete AML model has two effects. First, winds tend to blow from cooler to warmer SSTs, and while this affects the air humidity by small amounts (about 1 g kg^{-1} for typical advecting winds and humidity gradients), it has a correspondingly larger effect on the latent heat flux, which depends on the air–sea humidity *difference*. The SST simulated with the complete AML model is hence cooler in the trade wind regions and in the eastern Pacific where the winds bring drier air equatorward (see Boers and Betts 1988, for a discussion of the thermodynamics of cold advection off California).

The other effect relates to the diffusive flux, which is supposed to parameterize the effects of transients. This process operates to increase the relative humidity above its equilibrium value over the east Pacific cold

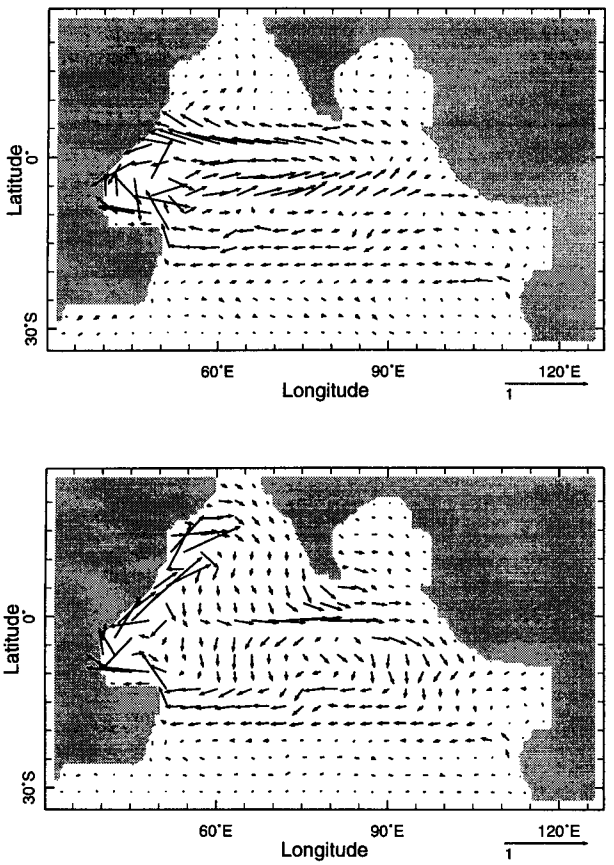

FIG. 14. Surface currents for February and August. The reversal of the Somali Current from boreal winter to summer is reproduced by the model with peak speeds of over 180 cm s^{-1}.

tongue. This occurs by mixing of higher humidity air from the north and south. Something like this actually occurs in nature and the relative humidity here is observed to be high (e.g., Wallace et al. 1989). The effect is to lower the latent heat flux and warm the SST. The dynamical model tends to create an overdeveloped cold tongue so this feedback is quite welcome. The local equilibrium heat flux scheme led to excessively cold SSTs in the cold tongue.

The importance of the nonlocal heat flux scheme was also seen in the Indian Ocean. Diffusive transports influenced the SST off Somalia where coastal upwelling creates large SST gradients. Off Australia and east of India dry advection was capable of cooling the SSTs by noticeable amounts.

Several workers have recently demonstrated that reliable simulation of the seasonal cycle of SST in the eastern equatorial Pacific requires a physically realistic treatment of ocean mixed layer physics (Chang 1994; Chen et al. 1994b; Wang et al. 1995). The important processes to capture are the variation of the mixed-layer depth, its dependence on surface buoyancy forcing and wind stirring, and the stability dependence of entrainment at the mixed layer base. Our experiments have used the hybrid mixing scheme of Chen et al. (1994a), which takes into account these effects. Nonetheless, serious problems remain in the simulation of the SST in the region of the Pacific cold tongue. Most serious is the excessively cold water during northern spring. The model fails to simulate the warming that

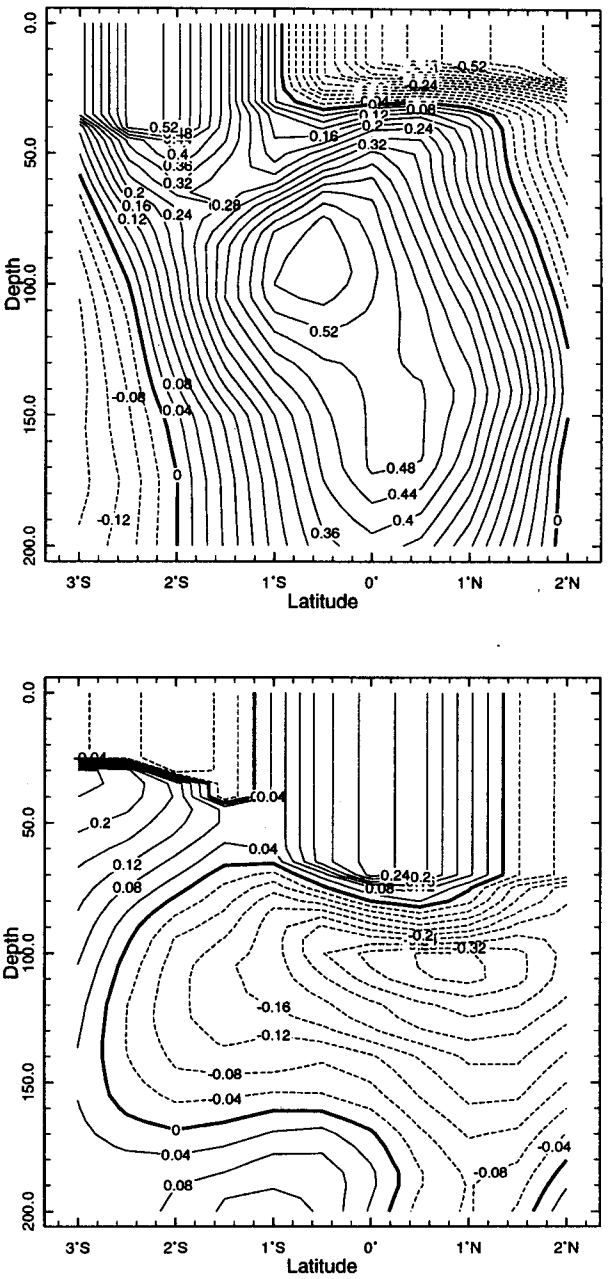

FIG. 15. A section of zonal currents along 58°E (contour interval 0.04 m s^{-1}) shows the Equatorial Undercurrent in February with core velocity of over 50 cm s^{-1}. Both surface currents and subsurface currents reverse directions in August.

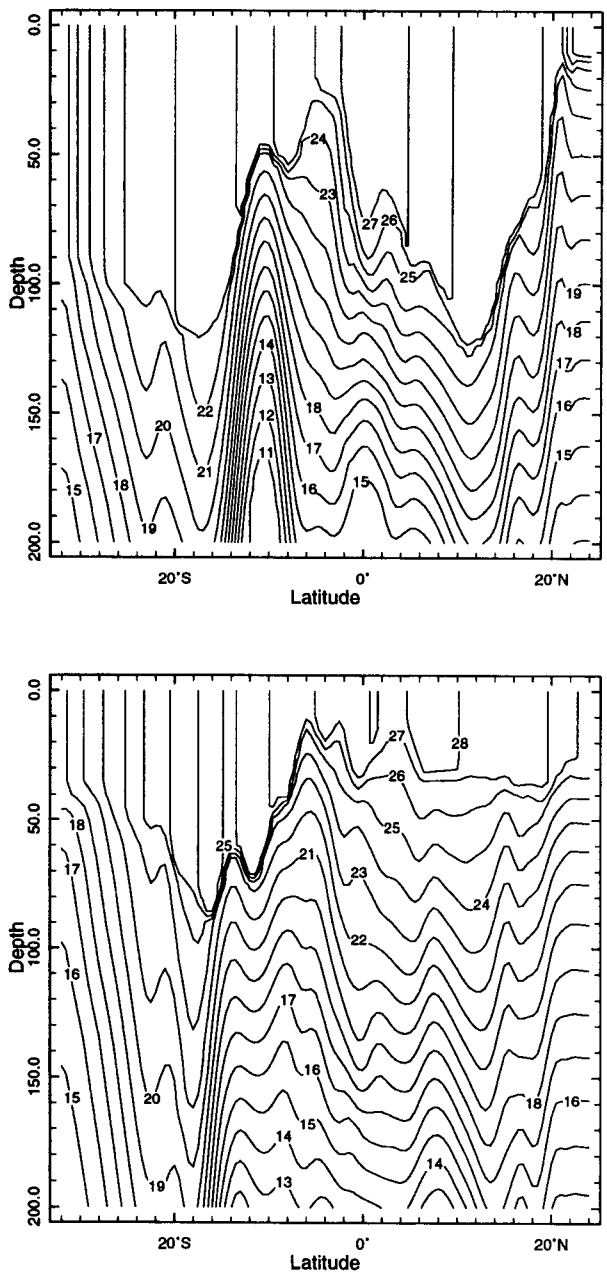

FIG. 16. A section of temperature vs depth in August and November along 60°E. The deep pool of warm water at 8°N is associated with the Great Whirl. The ridge at just north of 8°S is also seen observations.

occurs in nature at this time. The causes of this are likely complex. It is probably in part related to the simulation of the undercurrent. This extends too far east and too close to the surface. The velocity shear at the mixed layer base is large and the dynamical instability mechanism in the mixing scheme brings up cold water from below. This is probably a serious overestimate of the real entrainment. Apparently Chen et al. (1994b), using a very similar ocean model, but with a different surface heat flux scheme, did not encounter this problem.

The experiments we ran with a local mixed-layer model demonstrated some of the problems that can be introduced when using a variable depth mixed layer. In many areas of each ocean the SST errors became larger than found by Seager and Blumenthal (1994) using a similar local heat flux model, but a fixed depth mixed layer. The net production of TKE in a bulk ML formulation, such as the hybrid ML used here, is quite sensitive to the net surface heat flux. Positive feedbacks can occur between warming (cooling) of model SSTs and shallowing (deepening) of MLDs. With the nonlocal AML scheme for determining the surface fluxes this positive feedback is opposed by the horizontal fluxes of heat and moisture in the atmosphere that prevent development of small-scale features in the SST field (e.g., Seager et al. 1995b).

In ocean GCMs with active thermodynamics such as the one presented here, there are feedbacks between the dynamics and the thermodynamics. For example, in the eastern equatorial Atlantic and the Pacific, simulations with the local equilibrium mixed-layer result not only in colder SSTs but also deeper MLDs. This leads to weaker surface currents because the wind stresses are now acting on a thicker ML, which in turn affects the advective and upwelling terms in the heat budget. In addition, the thermocline slope is smaller resulting in an EUC that is up to 15% weaker. The mixed layer and its diabatic forcing play an important role in determining thermocline ventilation/subduction rates (Williams 1991) especially in the wind-driven subtropical gyres. The implication is that, when attempting to improve representation of near-surface mixing in ocean models, the surface buoyancy forcing should be accorded the same degree of attention. Once again it is the feedbacks between the fluxes and the SST that is critical. Some workers have attempted to improve mixed layer processes while fixing the atmospheric state (e.g., Blanke and Delecluse 1993). Assuming an invariant atmosphere is the opposite extreme to assuming local equilibrium and is also likely to effect the interactions between the mixed-layer processes and the surface fluxes. Reality lies somewhere in between: the atmosphere adjusts to the underlying SST, but not in a local sense.

5. Concluding remarks

An advective AML model has been coupled to a reduced gravity, primitive equation ocean GCM. The focus of this work has been to demonstrate that the seasonal variations of the SSTs can be reproduced without resorting to artificial flux corrections or relaxation to observations. Using the observed atmospheric state in the surface heat flux boundary condition is sometimes justified by arguing that this allows examination of the

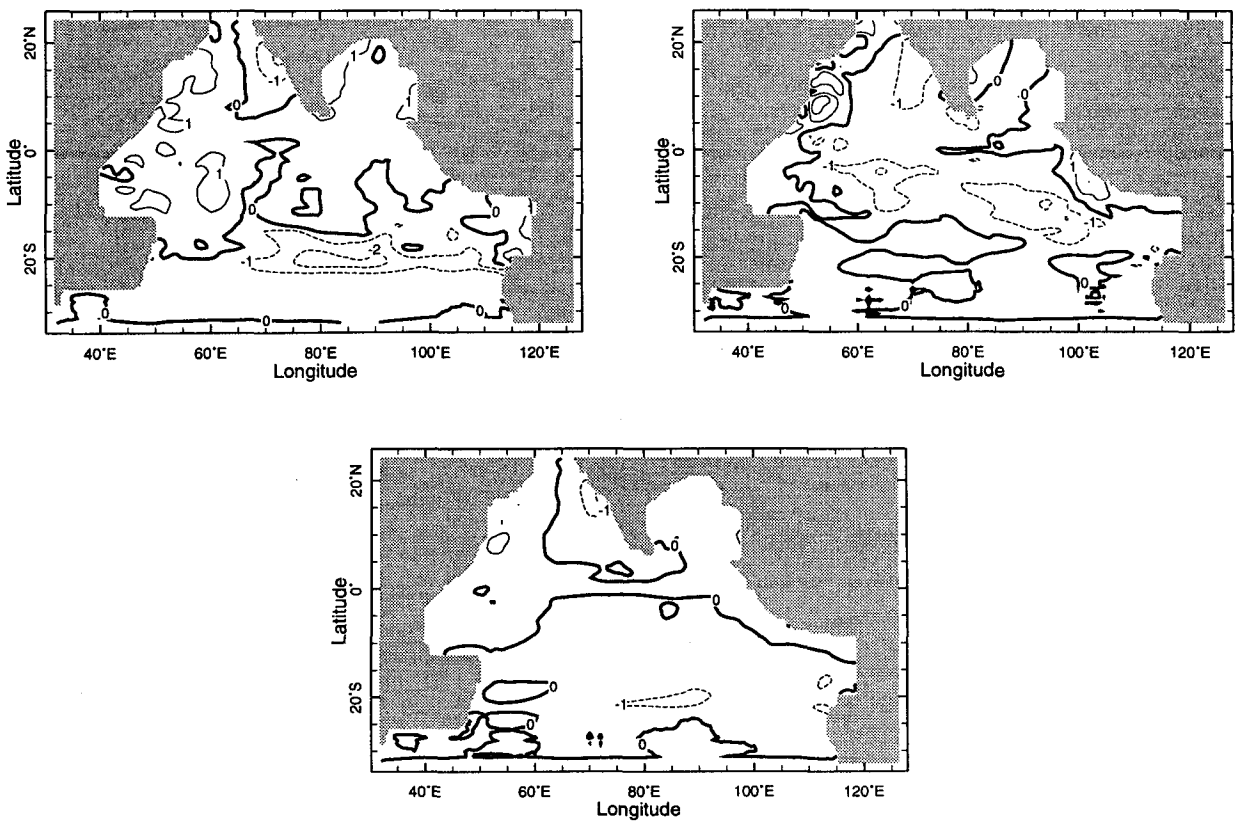

FIG. 17. Model SSTs with AML (contour interval 1°C): top panels show the differences between model SSTs and Levitus data for March (left) and September (right). The bottom panel shows the differences in annual mean Levitus and model SSTs.

SST the model would produce if the atmosphere was "perfect." However, this is not the case. A "perfect" atmosphere model, in this respect, is one that properly models the processes that relate the three dimensional transports of heat and moisture to the underlying SST. It is *not* one which, given an erroneous SST, returns observed values of air temperature and humidity since that would require an improper representation of the atmospheric processes. The implications are clear: running an ocean model with an imposed atmospheric state is a poor precursor to coupling. The imposed atmospheric state may be helping, in the face of ocean model errors, to force the SST to the observations, but as soon as coupling occurs even a "perfect" atmosphere model will cause the coupled state to drift away from observed. The only hope is to compute SST in an environment where the atmospheric processes that couple the marine boundary layer to the SST are properly modeled. Such a "perfect" atmospheric model will of course give surface fluxes that differ from the true ones if the SST is incorrect. This is the kind of procedure we adopted here. It allows easy identification of ocean model errors and increases confidence in the ability of the model to avoid severe climate drift when it is coupled to a complete atmosphere model.

Simulations of each of the tropical oceans are presented. Model SSTs compare well with Levitus climatological data over most of the model domains. The spatial and temporal behavior of the ocean circulation is also generally well simulated. The main, and serious, model flaw is an inadequate representation of the seasonal cycle in the upwelling regions of the eastern Atlantic and Pacific Oceans. In these regions the warming of SST around March and April is absent in the model which, instead, continues to entrain cold water from below. The causes of this problem are related to the simulation of the undercurrent and, hence, the vertical velocity shear, and to the simulation of ocean mixed layer processes. This is not the only GCM with this problem and the proper simulation of the interactions between surface buoyancy forcing and mixing in these climatically important regions remains a pressing issue in equatorial oceanography.

We have clearly demonstrated the usefulness of the nonlocal atmospheric mixed-layer parameterization for a proper simulation of surface fluxes and SST. The improvement in SST simulation, relative to a local heat mixed-layer model, that this scheme yielded was particularly marked in the Atlantic Ocean. This answers the question raised by Blumenthal and Cane (1989)

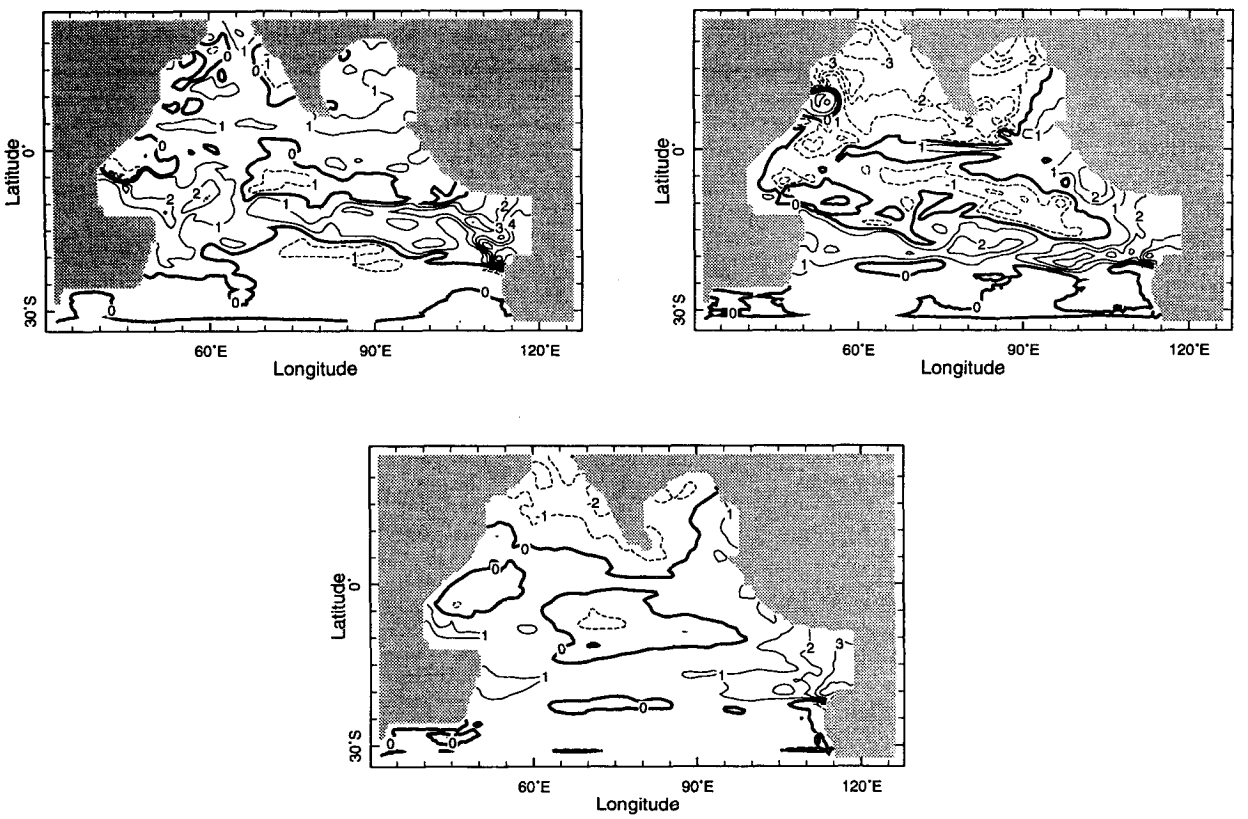

FIG. 18. Differences between model SSTs with a local equilibrium heat flux and Levitus data [contour interval 1°C: for March (top left), August (top right), and the annual mean (bottom)].

and Sennechael et al. (1994) as to what was the cause of the very large errors in SST they obtained with simplified ocean models. The error was in fact related to the assumption of local equilibrium between the SST and the marine boundary layer. The simple ocean model was apparently less responsible since our GCM performs just as poorly if we adopt a local heat flux parameterization. The discouraging conclusion of Sennechael et al. (1994) that simple ocean models are just not up to the task of modeling Atlantic SST now needs to be reexamined. Coupling of their simple ocean model with our atmospheric mixed-layer model may yield SST simulations comparable in realism to those here. The huge computational gain of using simple ocean models makes this an attractive proposition that needs to be further explored.

It was also demonstrated that using the atmospheric mixed layer model led to discernible improvement in the simulation of Pacific and Indian Ocean SST. In both cases, advection of drier air can enhance latent heat fluxes and, over the Pacific cold tongue, diffusion can create the observed relative humidity maximum that acts to suppress latent heat loss. Excluding the nonlocal processes in surface heat flux parameterization can amplify, through a positive feedback between buoyancy forcing and mixed layer deepening, the inaccuracies in the simulation of the ocean mixed layer processes. In the work with simple ocean models, the assumption of a fixed mixed layer depth prevented such a feedback from operating. Increased realism in the modeling of the ocean mixed layer increases the demand for realism in the representation of the surface heat fluxes. These considerations are unavoidable at higher latitudes where the local equilibrium assumption for the AML is much further from reality and the interactions between the mixed layer and the thermocline are more important. Model experiments for the extratropics are being carried out with the nonlocal heat flux scheme and will be reported elsewhere. The AML model is available as a modular FORTRAN subroutine and is easily incorporated into ocean models with no computational overhead with respect to other heat flux parameterizations. This makes it very attractive not only for comparison of model performance with the traditional heat flux formulations but also for various process studies.

Although we have raised a defense of simple ocean models, it should be remembered that these models need to specify the temperature of the water below the mixed layer and hence are not closed. Climate vari-

ability on decadal timescales or longer is presumably intertwined with the maintenance and variability of the tropical thermocline. Such issues cannot be addressed with the simple ocean models making GCMs, and other more complete models, a necessary tool for climate research. The success of the simple models in simulating SST has often been dismissed on the grounds that, by imposing the subsurface temperature, they are not doing the whole problem. The contribution of this work is that SSTs that are as good, or better, than obtained with simple models can be achieved in an environment where the thermocline structure is internally modeled, and in the absence of artificial constraints in the surface boundary conditions, just as long as care is taken in dealing with the interplay between SST and surface fluxes.

Acknowledgments. RS was supported by National Science Foundation Grant ATM92-24915. We would like to thank Dr. Yochanan Kushnir for his comments and criticism and Dr. Lawrence Rosen for letting us steal CPU cycles from machines under his care. We are truly grateful to the two anonymous reviewers whose valuable comments improved the focus of the paper. The surface heat flux parameterization discussed here is available as a FORTRAN subroutine and can be obtained from RS by sending e-mail to rich@seppie.ldeo.columbia.edu.

REFERENCES

Arakawa, A., and V. Lamb, 1977: Computational design of the basic dynamical processes of the UCLA general circulation model. *Methods Comput. Phys.*, **17,** 173–265.

Augstein, E., 1978: The atmospheric boundary layer over the tropical oceans. *Meteorology over the Tropical Oceans,* D. Shaw, Ed., Roy. Meteor. Soc., 73–104.

Betts, A., 1976: Modeling subcloud layer structure and interaction with a shallow cumulus layer. *J. Atmos. Sci.*, **33,** 2363–2382.

——, and W. Ridgway, 1989: Climatic equilibrium of the atmospheric convective boundary layer over a tropical ocean. *J. Atmos. Sci.*, **46,** 2621–2641.

Blanke, B., and P. Delecluse, 1993: Variability of the tropical Atlantic Ocean simulated by a general circulation model with two different mixed-layer physics. *J. Phys. Oceanogr.*, **23,** 1363–1388.

Blumenthal, M., 1990: Effects of west African air humidity on Atlantic sea surface temperature. *Greenhouse Effect, Sea Level, and Drought,* P. Paepe, R. Fairbridge, and S. Jelgersma, Eds., Kluwer, 21–40.

——, and M. Cane, 1989: Accounting for parameter uncertainties in model verification: An illustration with tropical sea surface temperature. *J. Phys. Oceanogr.*, **19,** 815–830.

Boers, R., and A. K. Betts, 1988: Saturation point structure of marine stratocumulus clouds. *J. Atmos. Sci.*, **45,** 1156–1175.

Busalacchi, A., and J. O'Brien, 1980: The seasonal variability of the tropical Pacific. *J. Phys. Oceanogr.*, **10,** 1929–1952.

Cane, M., S. Dolan, and S. Zebiak, 1986: Experimental forecasts of the 1982/83 El Niño. *Nature,* **321,** 827–832.

Cayan, B., 1980: Large-scale relationship between sea surface temperature and surface air temperature. *Mon. Wea. Rev.*, **108,** 1293–1301.

Chang, P., 1994: A study of the seasonal cycle of sea surface temperature in the tropical Pacific Ocean using reduced gravity models. *J. Geophys. Res.*, **99,** 7725–7741.

Chen, D., L. Rothstein, and A. Busalacchi, 1994a: A hybrid vertical mixing scheme and its application to tropical ocean models. *J. Phys. Oceanogr.*, **24,** 2156–2179.

——, A. Busalacchi, and L. Rothstein, 1994b: The roles of vertical mixing, solar radiation, and wind stress in a model simulation of the sea surface temperature seasonal cycle in the tropical Pacific Ocean. *J. Geophys. Res.*, **99,** 20 345–20 359.

——, S. E. Zebiak, A. J. Busalacchi, and M. A. Cane, 1995: An improved procedure for El Niño forecasting: Implications for predictability. *Science,* **269,** 1699–1702.

Cutler, A., and J. Swallow, 1984: Surface currents of the Indian Ocean (to 25°S, 100°E) (compiled from archived historical data). Rep. 187, Meteorological Office, 187 pp.

Gent, P., and M. A. Cane, 1989: A reduced gravity, primitive equation model of the upper equatorial ocean. *J. Comput. Phys.*, **81,** 444–480.

Giese, B., and D. Cayan, 1993: Surface heat flux parameterizations and tropical Pacific sea surface temperature simulation. *J. Geophys. Res.*, **98,** 6979–6989.

Gordon, C., and P. Corry, 1991: A model simulation of the seasonal cycle in the tropical Pacific Ocean using climatological and modeled surface forcing. *J. Geophys. Res.*, **96,** 847–864.

Halpern, D., 1987: Observations of annual and El Niño thermal and flow variations at 0°, 110°W and 0°, 95°W during 1980–1985. *J. Geophys. Res.*, **92,** 8197–8212.

Haney, R., 1971: Surface thermal boundary condition for ocean circulation models. *J. Phys. Oceanogr.*, **1,** 241–248.

Hellerman, S., and M. Rosenstein, 1983: Normal monthly wind stress over the world ocean with error estimates. *J. Phys. Oceanogr.*, **13,** 1093–1104.

Jensen, T., 1993: Equatorial variability and resonance in a wind-driven Indian Ocean model. *J. Geophys. Res.*, **98,** 22 533–22 552.

Kleeman, R., and S. Power, 1995: A simple atmospheric model of sea surface heat flux for use in ocean modeling studies. *J. Phys. Oceanogr.*, **25,** 92–105.

Knox, R., 1976: On a long series of measurements of Indian Ocean equatorial currents near Addu Atoll. *Deep-Sea Res.*, **23,** 211–221.

Kraus, E., and J. Turner, 1967: A one-dimensional of the seasonal thermocline. Part II. *Tellus,* **19,** 98–105.

Latif, M., 1987: Tropical ocean circulation experiments. *J. Phys. Oceanogr.*, **17,** 246–263.

Levitus, S., 1982: *Climatological Atlas of the World Ocean.* National Oceanic and Atmospheric Administration, 173 pp.

Li, Z., and Leighton, H., 1993: Global climatologies of the solar radiation budgets at the surface and in the atmosphere from 5 years of ERBE data. *J. Geophys. Res.*, **98,** 4919–4930.

Lorenz, E., 1971: An N-cycle time-differencing scheme for stepwise numerical integration. *Mon. Wea. Rev.*, **99,** 644–648.

Luksch, U., and H. von Storch, 1992: Modeling the low frequency sea surface variability in the North Pacific. *J. Climate,* **5,** 893–906.

Luyten, J., and D. Roemmich, 1982: Equatorial currents at semi-annual period in the Indian Ocean. *J. Phys. Oceanogr.*, **12,** 406–413.

McCreary, J., and P. Kundu, 1988: A numerical investigation of Somali Current during Southwest Monsoon. *J. Mar. Res.*, **46,** 25–58.

——, ——, and R. Molinari, 1993: A numerical investigation of dynamics, thermodynamics, and mixed-layer physics in the Indian Ocean. *Progress in Oceanography,* Vol. 31, Pergamon, 181–244.

McPhaden, M., and M. McCarty, 1992: Mean seasonal cycle and interannual variations at 0°, 110°W and 0°, 140°W during 1980–1991. NOAA Tech. Memo., ERL PMEL-95, 20–24.

Miller, A., J. Oberhuber, N. Graham, and T. Barnett, 1992: Tropical Pacific Ocean response to observed winds in a layered general circulation model. *J. Geophys. Res.*, **97,** 7317–7340.

Molinari, R., D. Olson, and G. Reverdin, 1990: Surface current distributions in the tropical Indian Ocean derived from compila-

tions of surface buoy trajectories. *J. Geophys. Res.*, **95,** 7217–7238.

Murtugudde, R., M. Cane, and V. Prasad, 1995: A reduced gravity, primitive equation, isopycnal ocean GCM: Formulation and simulations. *Mon. Wea. Rev.*, **123,** 2864–2887.

Nicholls, S., and M. LeMone, 1980: The fair weather boundary layer in GATE: The relationship of subcloud fluxes and structure to the distribution and enhancement of cumulus clouds. *J. Atmos. Sci.*, **37,** 2051–2067.

Oberhuber, J., 1993: Simulation of the Atlantic circulation with a coupled sea ice-mixed layer-isopycnal general circulation model. Part II: Model experiment. *J. Phys. Oceanogr.*, **23,** 830–845.

Philander, S. G., 1973: Equatorial Undercurrent: Measurements and theories. *Rev. Geophys. Space Phys.*, **11,** 513–570.

——, and D. Seigel, 1985: Simulation of the El Niño of 1982–1983. *Coupled Ocean–Atmosphere Models,* J. Nihoul, Ed., Elsevier, 517–541.

——, and Pacanowski, R., 1986: A model of the seasonal cycle in the tropical Atlantic Ocean. *J. Geophys. Res.*, **91,** 14 192–14 206.

——, W. Hurlin, and A. Seigel, 1987: Simulation of the seasonal cycle of the tropical Pacific Ocean. *J. Phys. Oceanogr.*, **17,** 1986–2002.

Price, J., R. Weller, and R. Pinkel, 1986: Diurnal cycle: Observations and models of the upper ocean response to diurnal heating, cooling, and wind mixing. *J. Geophys. Res.*, **91,** 8411–8427.

Rahmstorf, S., and J. Willebrand, 1995: The role of temperature feedback in stabilizing the thermohaline circulation. *J. Phys. Oceanogr.*, **25,** 787–805.

Rao, R., R. Molinari, and J. Festa, 1989: Evolution of the climatological near-surface thermal structure of the tropical Indian Ocean. *J. Geophys. Res.*, **94,** 10 801–10 815.

Reverdin, G., and M. Fieux, 1987: Sections in the western Indian Ocean—Variability in the temperature structure. *Deep-Sea Res.*, **34,** 601–625.

——, ——, J. Gonella, and J. Luyten, 1983: Free drifting buoy measurements in the Indian Ocean equatorial jet. *Hydrodynamics of the Equatorial Ocean,* J. Nihoul Ed., Elsevier, 99–120.

——, C. Frankignoul, E. Kestenare, and M. McPhaden, 1994: A climatology of the seasonal currents in the equatorial Pacific. *J. Geophys. Res.*, **99,** 20 323–20 344.

Richardson, P., and T. McKee, 1989: Surface velocity in the equatorial oceans calculated from historical ship drifts. WHOI Tech. Rep. WHOI-89-9, 50 pp.

Sarmiento, J., 1986: On the north and tropical Atlantic heat balance. *J. Geophys. Res.*, **91,** 11 677–11 689.

Seager, R., 1989: Modeling tropical Pacific sea surface temperature: 1970–1987. *J. Phys. Oceanogr.*, **19,** 419–434.

——, and M. Blumenthal, 1994: Modeling tropical Pacific sea surface temperature with satellite-derived solar radiative forcing. *J. Climate,* **7,** 1943–1957.

——, S. Zebiak, and M. A. Cane, 1988: A model of the tropical Pacific sea surface temperature climatology. *J. Geophys. Res.*, **93,** 1265–1280.

——, M. Blumenthal, and Y. Kushnir, 1995a: An advective atmospheric mixed layer model for ocean modeling purposes: Global simulation of surface heat fluxes. *J. Climate,* **8,** 1951–1964.

——, Y. Kushnir, and M. Cane, 1995b: On heat flux boundary conditions for ocean models. *J. Phys. Oceanogr.*, **25,** 3219–3230.

Sennechael, N., C. Frankignoul, and M. Cane, 1994: An adaptive procedure for tuning a sea surface temperature model. *J. Phys. Oceanogr.*, **24,** 2288–2305.

Shinoda, T., and R. Lukas, 1995: Lagrangian mixed layer modeling of the western equatorial Pacific. *J. Geophys. Res.*, **100,** 2523–2541.

Stockdale, T., D. Anderson, M. Davey, P. Delecluse, A. Kattenberg, Y. Kitamura, M. Latif, and T. Yamagata, 1993: Intercomparison of tropical ocean GCMs. World Circulation Programme Research, Memo. WCRP-79, 67 pp.

Swallow, J., 1967: The Equatorial Undercurrent in the western Indian Ocean in 1964. *Stud. Trop. Oceanogr.*, **5,** 15–36.

Wacongne, S., 1988: Dynamics of the Equatorial Undercurrent and its termination. Ph.D. dissertation, Massachusetts Institute of Technology, 94 pp.

——, 1989: Dynamical regimes of a fully nonlinear stratified model of the Atlantic Equatorial Undercurrent. *J. Geophys. Res.*, **94,** 4801–4815.

Wang, B., T. Li, and P. Chang, 1995: An intermediate model of the tropical Pacific Ocean. *J. Phys. Oceanogr.*, **25,** 1599–1616.

Wallace, J., T. Mitchell, and C. Deser, 1989: The influence of sea surface temperature on surface wind in the eastern equatorial Pacific: Seasonal and interannual variability. *J. Climate,* **2,** 1492–1499.

Williams, R., 1991: The role of the mixed layer in setting the potential vorticity of the main thermocline. *J. Phys. Oceanogr.*, **21,** 1803–1814.

Woodberry, K., M. Luther, and J. O'Brien, 1989: The wind-driven seasonal circulation in the southern tropical Indian Ocean. *J. Geophys. Res.*, **94,** 17 985–18 002.

Wyrtki, K., 1973: An equatorial jet in the Indian Ocean. *Science,* **181,** 262–264.

——, and B. Kilonsky, 1984: Mean water and current structure during the Hawaii-to-Tahiti shuttle experiment. *J. Phys. Oceanogr.*, **14,** 242–254.